Reply to reviewer 1

Review of "Quantifying sediment mass redistribution from joint time- lapse gravimetry and photogrammetry surveys, by Mouyen et al.

We thank the reviewer for his comments. Our answers are written in blue after each comment.

This paper describes a field effort to quantify sediment mass redistribution over three years at a study area in Taiwan. The study integrates, for the first time that I am aware, repeat microgravity and photogrammetry measurements. The paper is well written and needs minimal editing. The study has some limitations, most of which are noted.

The figures are well prepared and appropriate to the manuscript. There are a large number of them, perhaps some could be combined. For example, the gravity time series is shown in 3 different figures and a plan- view map is in 4 figures.
We combine Figures 7 and 8. We think more combinations may make the figure too complicated by stacking too much information.

Major comments:
1) The paper would be improved by considering the problem in a more general sense, in particular, the relation between mass change and the region of sensitivity of the gravimeter. For example, its not clear to me how mass redistribution on the hill slope affects the gravity change; mass moving down the slope, towards the gravity transect, would seem to cause a net decrease in gravity (i.e., the force of the mass is greater, because its closer to the gravimeter, but it's a negative change in gravity because mass is above the transect). Presumably this is handled implicitly in the least- squares solution but a more general discussion is warranted. Nowhere in the paper is the difference between mass change above and below the meter discussed.
Yes. We now elaborate on that point in lines 100-126 together with two new subpanels (e) and (f) in new figure 2 (ex-figure 1 in the manuscript you reviewed). The new subpanels clarify the influence of both the angle and distance from the gravimeter. We also compute a synthetic gravity effect using the actual topography of the studied area, to give a better understanding on how each mass (each pixel of the DEM) influence the gravity at one of the RG site.

2) I disagree with the reliance on improved, future gravimeters to justify the work. For one, they are far from a successful field demonstration, much less buried underneath a stream channel. Constraining instrument drift in that environment would seem impossible. Second, the FG- 5 absolute- gravity meter (and even the A- 10) provides accuracy quite sufficient for this type of study, given the uncertainty in the other parameters. I think it would be more effective to investigate further what could be learn using a dense network of gravity stations, and/or using a network of combined relative/absolute measurements to reduce uncertainty (gravity- change uncertainty of 3- 4 uGal should be possible).
About the new gravimeters: Recent literature in high-impact journals shows that gravimetry is undergoing significant progress through the development of a variety of new devices using

leading edge technologies. We believe it is appropriate to trust such messages by forecasting potential applications and making some quantitative assessment, even if, indeed, not all prototypes are perfect yet. However, that is not the main purpose of the paper, rather a perspective that we confine to the discussion. The main purpose is a quantitative estimation of sediment mass redistribution, which is still a challenging task.

About the network densification: Yes, having a denser network of gravity stations will be useful, but only if we can make measurements in the active bed channel of the river. Adding more stations along the river or more inland will not bring better constraints, because they remain too far from where mass redistribution actually occurs. But measuring gravity in the active bed channel, using CG5/FG5/A10, requires long lasting sites at the surface of this channel, which is impossible due to the dynamic of the sediment of the channel. That is why we investigate the effect of a buried gravity network, in the active bed channel. MEMS gravimeters are the only rational option in this case even though, we agree, they are still under development. This is discussed in section 6.3 and 6.4.

3) The introduction provides a broad overview of erosion and surface processes, but nothing on why measurements of sediment mass are important, rather than just sediment volume. Is sediment mass (or mass flux) an important parameter in landslide or sediment transport models?
Yes, we now elaborate on this in lines 50-62 by pointing out the extensive use of sediment mass rather than volumes both in models and field observations.

Given that sediment density is readily measured from soil samples, volume is accurately measured from photogrammetry, and the density estimate from gravity is relatively uncertain, what is the big advantage of gravity measurements? (for one, they can be used where site access is prohibited or dangerous, e.g. volcanos)
The advantage is that gravimetry measures a mass. Photogrammetry is purely geometric and sediment density sampling is extremely local. Here, we did the density measurements just for comparison. Joint photogrammetry-gravimetry survey should in fact provide a better average density, because the gravity signal integrates mass contribution over the entire survey. Density samples are local measurements over a heterogeneous body of material, they cannot sense the average density as well as gravimetry. The point of using gravimetry/photogrammetry is to not have to measure the density of soil samples. Such samples are likely to bias mass estimates because they are local and not necessarily representative of the heterogeneity of the area. On the other hand, the mass effect measured by gravity already averages this heterogeneity density and thus, is more reliable. We modify lines 61-62 and lines 387-390 to better clarify this point.

4) Relying only on global hydrology models is a major shortcoming. The river level varied by over 1m between surveys, indicating groundwater- level changes were also large. The gravity effect of this local change is likely as large or larger than the global changes, but is ignored completely. There is likely large storage changes in the unsaturated zone, and possibly a variable rain- shadow effect at each station (i.e., the gravitational effect of soil-moisture change is different at each station, even if the soil moisture change is the same).
We agree that global hydrological models are not perfect, but we could not make a dedicated hydrological model for this area by (trying to) reconcile the rainfall measurement and the river water level. As a matter of fact, the river water as no data in 2017 and is indeed

about 1 m higher in 2016 than in 2015. The MERRA2 model, which has improved at estimating water storage changes estimated from space gravity measurements (Reichle et al. 2017), also shows an increase of +3 microGal from 11/2015 to 11/2016 (Figure 5). Stating that +1 m of river level corresponds to +1m of groundwater table rise and assuming that the porosity of the ground is 10%, then, 1m of groundwater table correspond to a layer of 10 cm water. That is equivalent to +4 microGal under a Bouguer plate approximation, which is acceptable compared to MERRA2's +3 microGal. Indeed, it is better to have a local hydrogravity model for such corrections, but this requires continuous gravity measurements for at least a few years, ideally with groundwater level monitoring (e.g. Mouyen et al. 2016). We cannot do that here. Relying on global models is also the reason why we add large uncertainties on this hydrological correction.

- Mouyen, M., Chao, B. F., Hwang, C., & Hsieh, W.-C. (2016). Gravity monitoring of Tatun Volcanic Group activities and inference for underground fluid circulations. *Journal of Volcanology and Geothermal Research*, *328*, 45–58. https://doi.org/10.1016/j.jvolgeores.2016.10.001
- Reichle, R. H., Draper, C. S., Liu, Q., Girotto, M., Mahanama, S. P. P., Koster, R. D., & De Lannoy, G. J. M. (2017). Assessment of MERRA-2 land surface hydrology estimates. Journal of Climate, 30(8), 2937–2960. https://doi.org/10.1175/JCLI-D-16-0720.1

5) Data are available by contacting the author. I believe this is against the spirit, if not the letter, of the journal: "Copernicus Publications requests depositing data...in reliable (public) data repositories..." I would strongly prefer the data were made available online. Certain aspects ofthe manuscript, such as measurement uncertainty, were difficult to evaluate without access to the data. If some data are published by others (e.g., stage and sediment data provided by the Taiwan Water Resources Agency) you should provide as precise a reference/URL as possible. I looked on the WRA website but found no data for the Laonong River.
Yes, we now provide all data in a public archive file (Data availability section). Indeed, the links to the webpage of WRA was missing, we add it in the references and in the data archive. Here is one link for 2015. All reports (pdf) are at http://gweb.wra.gov.tw/wrhygis/

Minor comments:
The review copy lacked spacing or indentation between paragraphs, making reading difficult.
We improve spacing.

51: This line ("The surveys were done...") seems out of place. Perhaps split off the description of the study area/data from the paragraph about surface processes.
Yes, we rearranged.

Intro: Suggest discussing the 1- d simplification often used in hydrology and why it can't be used for 3- d surface processes.
Yes, we now discuss this on lines 91-97.

68: Are you using the point mass approximation for all of the forward gravity modeling? Are you sure that's appropriate for the nearby prisms (please state that, if so). Consider using the Leiriao (2009) approach that uses the prism/McMillan/point mass formulas, depending on distance.
No we don't use point mass approximation for all of the forward gravity modeling. Lines 99-126 aimed to introduce the concept of gravimetry in its simplest form (point mass) just to

stress the importance of the mass, distance and angle between the measurement site and the mass. The computations are done by rectangular prisms method (line 361). We rewrite this paragraph more clearly and introduce the prism method as well already here to remove confusion (lines 100-126). Several methods exist to model gravity but rectangular prism is the most appropriate in our case, because the gravity effect is modelled from surface changes measured by photogrammetry and returned as regular grids of elevation.

70- 75: Suggest discussing the importance of the horizontal angle, and the relative effect of mass change above and below the gravimeter.
Yes, this is now done both in lines 100-126 and in the new panels of new Figure 2.

74- 76: These lines seem out of place. Move to the conclusion?
Indeed. We don't move it to the conclusion but we rephrase it earlier in the introduction, lines 82-85.

84: The exact location…
Ok.

84: How long were the GPS occupations, and what is their estimated precision? RTK indicates they may have been as short as a few seconds. In that case I would expect the vertical precision to be on the same order as the indicated vertical movement. I.e., you may be adding noise to the data rather than correcting for elevation change.
The GPS-RTK occupations last for 30 minutes and returns standard deviations ranging from 3 to 7 mm. They are only used to get an exact horizontal location of each site. This allows to locate each site relative to the photogrammetry data, all referenced in the coordinate reference system TWD97, using the Taiwan Datun 1997. Then the vertical position is taken from the photogrammetry data. But the vertical displacement at each site is assumed to be identical to that measured at the permanent GPS site (PAOL). The rapid uplift at PAOL is due to active tectonic processes at work in Taiwan. There is no evidence for active faults across the gravity network, so the entire area can be assumed to experience the same uplift rate. We clarify lines 259-263.
4 cm of motion over a year is a lot in this environment – is there an indication why there is so much movement?
(Please note that Figure 4 shows almost 4 cm uplift over three years, not one).
Indeed it is quite a high rate (more than 1 cm/an) and it is due to the large tectonic uplift at work in Taiwan (eg Ching et al., 2011). We add this information in section 2, lines 259-263.

- Ching, K.- E., M.- L. Hsieh, K. M. Johnson, K.- H. Chen, R.- J. Rau, and M. Yang (2011), Modern vertical deformation rates and mountain building in Taiwan from precise leveling and continuous GPS observations, 2000–2008, J. Geophys. Res., 116, B08406, doi:10.1029/2011JB008242.

87: "are not plain" is unclear. Do you mean they are not present?
The meaning is that they are not one solid/closed block, so we can crawl inside (see Figure B1a). We simplify the sentence to: "This dolosse storage also covered BA03 and BA04 but those two sites could still be measured" (line 137-138)
Change "will be" to "was".
Ok.

88: If measurements began in 2006, are there several more data points that could be shown on fig. 3?
There are more measurement indeed but Morakot typhoon in 2009 and its subsequent massive landslides somehow reset the whole area. The gravity offset before/after Morakot is about 30 microgal, thus the continuation from data before 2009 to present is irrelevant. The measures from 2009-2010 were not used either because too much reconstruction work was ongoing at that time, taking out debris from the river, thus interfering with natural sediment redistribution. The point of referring to the "history" of AG06 study is that thanks to it, we know that sediment redistribution can be well observed at this location using gravimetry.

Along with major comment 1, consider revising the methods section to present more prominently the "big picture": a least- squares inversion to determine sediment density. As written, you jump directly into the details of the gravity surveys. It might just require a short introductory paragraph in Methods.
Ok. We have added an introductory paragraph on lines 179-183.

Also, you could move the Study Area information after Methods – what's important is the development and demonstration of the method, not the details of a particular study area.
We prefer our original plan because it is easier to describe the method when the basic features of the site have been introduced. Also we want to keep the continuity Method -> Results -> Interpretation.

122: Was the drift correction first- order linear? I would be interested in the statistics of the adjustment. Measurement uncertainty (i.e., a posteriori standard deviation from the network adjustment, which accounts for the measurement uncertainty at each station) doesn't appear to be included in Table 1?
Yes it is linear. We add a new Appendix A with details on the gravity survey processing. Table 1 summarizes all corrections without the drift, because the drift estimation is altered by the tides, polar motion and air pressure corrections, hence by their uncertainty. Indeed, these corrections are applied before the adjustment. We add the measurements uncertainties in a new Table 2.

Typically earth tide and ocean load, possible atmospheric pressure, corrections would be applied to the relative gravity measurements prior to the network adjustment, and therefore their uncertainty would be included in the a posteriori standard deviation. Other corrections (ground motion, hydrology) would be applied after the network adjustment.
Yes, we add a column in table 1 that specifies when is each correction applied, before or after the adjustment. We also update the text at lines 250-253.

175: What's the estimated vertical accuracy of the photogrammetry? Fig. 8 suggests it might be pretty low; there are a lot of orange and blue pixels (+/- 5 m) outside of the landslide area in areas that presumably had little elevation change. Does uncertainty in the photogrammetry influence the density determination?
Outside of the landslide area, the terrain is covered with tropical vegetation. The surface of the vegetation is no well handled by photogrammetry. This area is also inaccessible, it does not contain ground checkpoints or some ground structures (buildings, roads, bridge). This adds uncertainty to the photogrammetry data in this area. But for the riverbed and the landslide areas (no vegetation, stable structures and control points), the uncertainty is small

(2-5 cm). Shifting the height of the rectangular prisms by +/- 5 cm has less than 1 microGal effect.

225: Given that you go into a lot of detail on least squares, it may be nice to mention in the A matrix that each row represents an observation and each column a density to solve for.
In fact, there is nothing to solve in the design matrix A, all its elements are known and they are neither direct observations nor densities. Matrix A links observation (L) and unknown densities (X). It could be built only thanks to the photogrammetry data and the expected gravity computed from it for a random density (set to 1), which the least-square inversion will adjust.

The A and X matrices seem incomplete: the two elements in the bottom right of A should be in a 4 th column, and ρ l in X should have two parts, ρ 1615 and ρ 1716 (?)
No because we invert a constant density of the landslide from 2015 to 2017. Indeed, the mountain remain made of similar material. On the other hand, the sediment in the river may not, because they are material taken from different location in the mountain range.

233: The text and figures indicate the gravity station is AG06 and the GPS station is PAOL. Suggest using “AG06” in the equations. Or better, rename it BA10 – the method of measurement isn’t important to the interpretation.
Right, we correct, all PAOL shall be AG06 in this case. We only use PAOL when we specifically refer to the GNSS station. We prefer to keep AG06 as it is the “official name” of the site, as labelled on the site itself.

254: Delete ’s from 2017’s
Ok.

254: Care to comment on the effort required to take density samples vs. gravity surveys? Do they provide the same information? How does their uncertainty compare?
Yes it took more effort. It is the same physical parameter, a total mass per unit of volume, water included. However, the sampling is local, while gravity, hence the density inverted from it, is integrative/averaged over the studied area. We add this in the text, lines 387-390. We did not assess the uncertainty.

257: Since “the density sample illustrate the variety of materials carried by the river and the landslide,” implying you took samples in both areas, why don’t you present the results for each area, instead of just the average?
We are not sure to understand this comment. Figure 8 (ex-Figure 9) does show the results of the density sampling in each area. But for the result of the gravity inversion, we use an average density because that is what the gravity measurements assesses. It is impossible to invert a high-resolution distributed density from the gravity measurements, since it is a too unconstrained system to solve. Even if gravity was measured at the place where the density sampling is done, the gravity signal would still be influenced by all densities around. Thus we at most define 2 areas, one of which being assessed twice, between 2015 and 2016 and between 2016 and 2017.

261: A wrong site location? How could that happen? Surely there are other explanations beyond just bad data: heterogeneous sediment density, underwater topographic change near these stations…
This is only a possible explanation, photogrammetry and site location were not originally done in the same reference frame, so one has to convert the site location to the photogrammetry reference frame. Also, gravity being an integrative measurement, local sediment heterogeneity will be smoothed by other densities. Water/underwater is a good candidate indeed, we rephrase accordingly, lines 398-399.

263: Suggest deleting: "...showing the interest...of the redistributed materials" – doesn't say much.
Ok.

269: delete "three"
Ok.
The large amount of overlap on the error bars on the densities shown in figure 2 would suggest the method can't really differentiate between river and landslide density. Also, 1.6 is very very low density and doesn't seem justified given the data in fig. 9.
Yes, we have discussed this a few lines above in the manuscript (lines. 387-390). Density 1.6 is quite low indeed but it could be because the river (density 1) was closer to the gravity sites in 2016, hence lowering the average density of the river sediments. We discuss this issue in section 6.2.

285: Is there any literature that discusses how landslide deposits change density as the landslide evolves? Is it reasonable to expect density increases in the downslope direction?
In earlier computations, we have tested to invert variable landslide densities but it returned inconsistent results (large uncertainties, negative densities). The main reason is that, as we wrote on lines. 382-384, the landslide is further from the gravity sites than the river, thus has a lower effect on the gravity changes. This appears already in inversion cases 2 and 3, where the overall landslide density has large uncertainties. About the density changes in the landslide, we could not find any literature on the subject. Nevertheless, if a density distinction should be done, we believe it would be better to separate the density of the removed materials (which are consolidated mountain material, high density) from the density of the stacked landslide material, which are piled up in coarse order and granulometry, surely leaving a lot of empty spaces between them (low density).

6.2: This analysis, to account for the effect of water in the river, seems like it should have been part of the data processing, as its removing a part of the gravity signal that you're not interested in. I don't understand why you would just assume the meter is 1- m deep at every location. Since you know the river stage during each survey (fig. 13), and its lowest in 2015, shouldn't you use the actual change in stage between each survey (a little over 1 m from 2015 to 2016, and 0.3 m from 2016 to 2017)? If cells were dry in 2015 and wet in 2016 you could estimate the elevation of the cell bottom (i.e., the land surface) from the photogrammetry. Assuming for the minute this analysis is correct, the corrected sediment density is 1.7 – this doesn't agree too well with your sediment samples?
We change lines 472-473. We make the distinction between wet sediment and pure water. See figure R1, the volume of water in the river cannot be estimated because the

photogrammetry cannot see the bottom below the river while both the river and sediment distribution are changing in time.

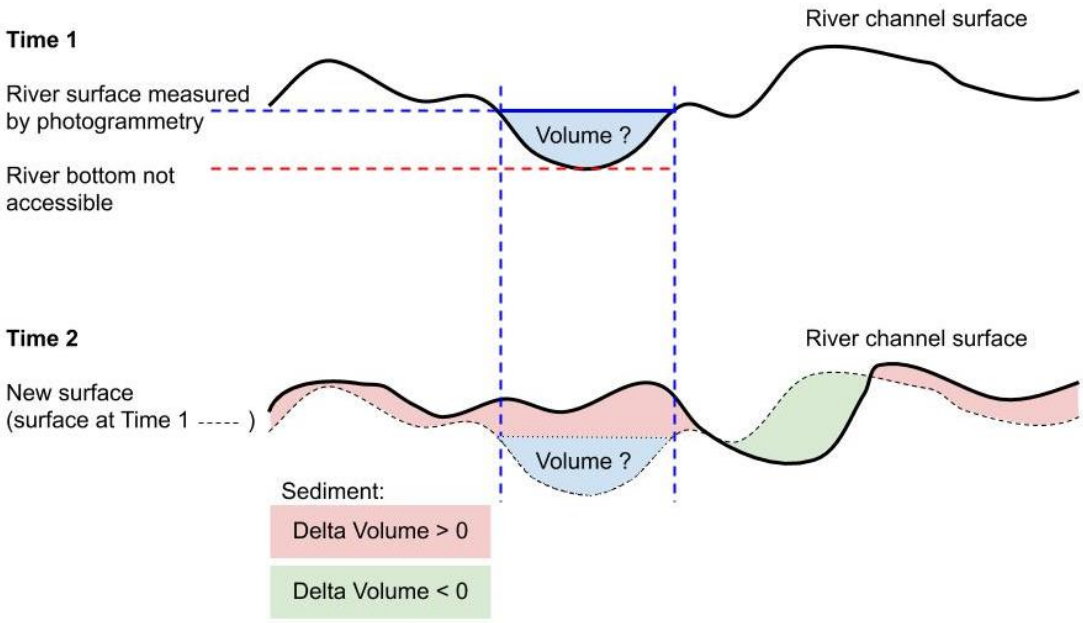

Figure R1: Cross section in the river bed at two different times, it is not possible to recover the bottom of the river, hence our 1-m assumption.

Therefore, there is no reference level for the river (water only) object hence no clear possibility to make a distinction between the materials “sediment” and “water”.
In fact, as we wrote in a reply above, it is not an issue that the density of the sediment samples does not agree with the estimated density. We now explain on lines 387-390 that the average density of the in situ samplings does not have to be close to the estimated densities, because we cannot sample the entire area, yet this area is made of heterogeneous material. The density estimated from gravity-photogrammetry inversion is in fact the best average density.

318: Delete “Eventually”
Ok.

328/332: use either density inversion or density- location inversion.
Ok, changed to density inversion.

342: You acknowledge that you would have better data with a more extensive gravity network, which is good, but you would still need some constraints on geometry to identify mass redistribution. Gravity change alone is insufficient.
Yes, we did not forget the need for geometrical constraints (lines 510). With a dense gravity network, we could restrict the geometry to the river only (it’s contour). The inversion procedure proposed by Camacho et al., 2011 can recover the density distribution in the (inaccessible) subsurface, hence without knowledge of the geometrical distribution of the masses. We agree that several geometries/densities may fit, not a unique one. But this could be assessed by interpretation and discussion.

- Camacho, A. G., Fernández, J., & Gottsmann, J. (2011). The 3-D gravity inversion package GROWTH2.0 and its application to Tenerife Island, Spain. Computers & Geosciences, 37(4), 621–633. https://doi.org/10.1016/j.cageo.2010.12.003

346: I don't think there's any advantage to a permanent quantum gravimeter vs. a permanent FG- 5.
Permanent FG-5 is not possible. The "most continuous" FG-5 series are done at few days to month frequency (Jacob et al. 2010) and require a nearly constant control from operator and not for longer than one year. Decadal FG-5 series exist but measurements are usually done once a year (Olsson et al. 2019), which is not our interest in the discussion. Hence the interest in absolute quantum gravimeter (AQG), which is rigorously absolute and continuous, and does not require as much operating effort as a FG-5.

- Jacob, T., Bayer, R., Chery, J., Jourde, H., Le Moigne, N., Boy, J.-P. J.-P., … Brunet, P. (2008). Absolute gravity monitoring of water storage variation in a karst aquifer on the larzac plateau (Southern France). J. Hydrol., 359(1–2), 105–117. https://doi.org/10.1016/j.jhydrol.2008.06.020
- Olsson, P.-A., Breili, K., Ophaug, V., Steffen, H., Bilker-Koivula, M., Nielsen, E., … Timmen, L. (2019). Postglacial gravity change in Fennoscandia—three decades of repeated absolute gravity observations. Geophysical Journal International, 217(2), 1141–1156. https://doi.org/10.1093/gji/ggz054

Much remains to be seen regarding the quantum and MEMS instruments. I would be much more interested in a discussion of what's possible with present- day instrumentation (combined absolute/relative measurements to improve accuracy, SG meters for continuous observation, maybe even borehole instruments)
Yes, but we mostly want to emphasize and promote the development of such instruments. Right now, MEMS only see tides, so yes, much remains to be seen. But any earlier progress in gravimetry has started with this observation. The improvement of this technique will also be positively correlated to the demand for such devices, hence the need to promote them. Combined absolute/relative is what we did and we discuss a new kind of absolute(AQG)/relative combination(MEMS).
SG meters are indeed permanent and we mentioned them as an alternative to AQG (line 513). However, unlike the AQG they are not transportable and, although slowly, their records drift in time, so they require regular drift estimation by using absolute gravity measurements (FG-5) in parallel.

6.4 I was a little confused by this section, you claim that you could quantify sediment discharge if bedload is at least 12.5 cm thick, as that is the amount required to provide a sufficiently large signal. But, in that case are you not just measuring the bedload, not total sediment discharge? A stream carrying 12.5 cm of bedload is likely carrying a significant amount of suspended sediment as well, but that would cause only a small gravity signal. Therefore, you might be able to measure bedload using gravity but not total sediment discharge.
The figure 12b shows the total gravity effect for suspended + bedload. 12.5 cm of bedload will create 10 microgal for suspended sediment concentration up to 5000 ppm, then for this same bedload, increases of sediment concentration will measurable, because the bedload effect is already 10 microGal. But we do not know how large will be the suspended sediment load (in particular, if it will be greater than 5000 ppm) as a function of the bedload. We add this text on lines 562-563.

Furthermore, since you are only measuring the change in bedload, you would need much more frequent surveys, or continuous data, to identify anything.
Yes, all computations in section 6.4 are meant for continuous gravity data (line 497). We recall this condition on lines 532 and line 536.

360: Change “measuring” to “estimating”
Ok.

375: Change “should” to “would need to”
Ok.

376: Change “strong” to “concentrated”
Ok.

387: You imply 10 μGal is the expected accuracy of a gravity- change measurement with today’s gravimeters, but that’s misleading. Sub- 5 μGal accuracy is typical for surveys using combined absolute/relative measurements, especially if multiple absolute- gravity stations are measured. Most of the uncertainty in this study is from uncertainty in the hydrology correction.
To our knowledge, the sub-5 microgal accuracy is not typical but rather the best achievable accuracy. It is achieved for laboratory conditions (Merlet al. 2008; Christiansen et al. 2011) or low-tectonics areas, such as Africa (Pfeffer 2103) or the Larzac Plateau (Jacob et al. 2010), mostly to investigate hydrological processes as those are the only significant mass redistribution occurring there. Taiwan is more noisy (microseismicity, anthropic noise, noise from river transport itself), and our data have 7 microGal uncertainty. This uncertainty of 10-microGal is taken as a threshold value. Nevertheless, it is true that the uncertainty from the hydrological correction is a problem. We rephrase lines 563-565.

399: Can you justify this work based on the value of sediment mass data, vs volume?
If the goal is estimates of “sediment redistribution” it seems that the photogrammetry would be sufficient for that.
Yes, this is now done on lines 50-62. We now use “sediment mass redistribution” instead of “sediment redistribution” whenever possible in the paper.

References:
There are a lot of references, many of them minimally relevant. The list could be shortened quite a bit.
We try to use the most appropriate references; we are unsure about which of them are considered irrelevant.

Titles should be lowercase, e.g., Carbone et al.
Ok.

IES- AS: Include the URL.
Ok.

600: Delete *
Ok.

Appendix B: If you think this is useful information, it would be worth elaborating. Its an interesting approach, one I hadn't seen before. I suggest either explaining it completely or just including it as a single sentence in the main text.30- 40 cm depth is a rather large hole, often density samples are taken from a 5cm x 5cm pit.
We rewrote Appendix B with more details. Here we dug a bigger hole because the balance needs a few kilograms to be reliable. The photogrammetry will also be more reliable.

Did you calculate wet bulk density? I assume so, as oven- drying is not mentioned. Typically density is reported for dry material.
Yes. We compute the in-situ density, since it is the one that influences the gravity measurements.

Step 3 is unclear, you mean that you should weigh the sediment (subtracting the weight of the bucket) and divide the sediment mass by the sediment volume.
Yes, we rephrase more clearly.

Reply to reviewer 2

We thank the reviewer for his detailed comments. Our answers are written in blue after each comment.

The paper presents a study of river induced mass transports from micro-gravimetry compared to volume changes inferred from photogrammetry. While I cannot assess weaknesses in the geometrical approach, the gravimetry part and its interpretation lacks serious shortcomings.

Gravity changes measured at 3 epochs are presented, consisting of gravity surveys with one relative gravimeter referred to point (AG06) observed with the absolute gravimeter (AG) FG5-224. However, the third epoch in 2017 has no reliable reference as the AG measurement failed. Instead, simply a mean value of three epochs was assumed, which is inadequate for the following reasons:
a) Figure 5 shows significant annual variations due to changes in the water storage, with a large uncertainty documented by the discrepancy of two selected models. Figure 3 documents AG observations in the range of 7 µGal from 2014 to 2016 which serve as a reference, where the first one was acquired in the beginning of the year (~Feb, not further specified in the paper), while the other two were measured in Nov (presumably in temporal proximity of the relative surveys, which should be documented).
This issue is described in the text (lines 213-221) along with a description of our assumptions before going on with an AG value in 2017. As we wrote, we could cancel the entire 2017 survey. This would not alter the conclusions of the paper, saying that combining photogrammetry and gravimetry helps quantifying sediment mass transfers. Indeed, the 2015-2016 gravity changes return very good results and they do not depend in any way to the 2017's AG.
Nevertheless, we took the chance to interpret the 2016-2017 surveys under simple but clearly stated assumptions. We agree that the AG value proposed for 2017 is a matter of discussion, since there is rigorously no way to know it. Thus, making a simple guess based on the mean of the previous values is appropriate. Also, looking backward, a posteriori results show a good consistency with this absolute value. We agree that hydrology has a significant effect on the measured value but we propose a way to deal with this effect (lines 265-279). This correction is also applied to the fictive 2017 AG value.
We add the exact timing the caption of Figure 3 and write that absolute and relative measurements were done at the same time (line 188).

b) As shown with Figure 5 a significant gravity decrease has to be considered from November to March. Although a "strong annual periodicity in this area" (L114) was

stated by the authors, this variability was not taken into account when approximating the missing absolute gravity reference value for 2017.

The strong annual periodicity means that the largest amplitude should occur for gravity values measured at a 6-months interval, specifically between summer (wet season) and winter (dry season) for the Taiwan region. Thus, when making measurements at a 12-months interval, this strong variability must theoretically not be taken into account. Nevertheless, as shown in Figure 5, the hydrological effect is seasonal but not rigorously sinusoidal. Some variability is expected and that is why we also correct the fictive 2017 AG value from hydrological effects. By doing the surveys in November (dry season), we expect this variability to be minimal.

c) With Figure 4 a clear vertical uplift of ~25 mm is documented for AG06 for the period 2015-2017 which corresponds to a gravity change of -5(!) µGal, assuming the ratio of -2 µGal/cm used by the authors (L153). The other AG surveys at AG06 since 2006 (L88) are neither documented nor used in this study, although a significant contribution must be expected for the extrapolation of the missing 2017 value. The assumption of the 2017 reference value seems therefore highly questionable.
Concerning the vertical displacement, since we only compare gravity values in 2015, 2016 and 2017, it is enough to work with a GNSS time series starting in 2015. Previous uplift will not have any influence on the corrections of gravity values. About using a longer AG time series, we agree that we could theoretically use the whole time series since 2006 to better extrapolate the 2017 value. But we didn't because Morakot typhoon in 2009 and its subsequent massive landslides reset the whole area. The gravity offset between Nov. 2008 and Nov. 2009, i.e. before and after Morakot, is about 30 microgal and is due to large sediment redistribution in this area (Mouyen et al. 2013). Sediment redistribution due to Morakot was such an exceptional event, with a significant impact on gravity, that it must not be included in the extrapolation of the 2017 gravity value, neither from mean nor from trend. The measures from 2009-2010 were not used either because too much reconstruction work was ongoing at that time, taking out debris from the river, thus interfering with natural sediment redistribution. We update the manuscript (lines 221-227) to include this point and remove ambiguities on the use of older gravity data.

- Mouyen, M., Masson, F., Hwang, C., Cheng, C.-C., Le Moigne, N., Lee, C. W., … Hsieh, W.-C. (2013). Erosion effects assessed by repeated gravity measurements in southern Taiwan. Geophysical Journal International, 192(1), 113–136. https://doi.org/10.1093/gji/ggs019

Furthermore, no uncertainty estimate is provided, and the uncertainty estimates for the individual FG5 observations in Fig. 3 doesn't seem to include systematic effects.
We disagree with this comment. The uncertainties of the FG5 observations are plotted in Figure 3 and taken into account together with the uncertainties listed in Table 1 and described in the text (lines 230-286) when computing all gravity changes for each survey. We add that the uncertainties shown in Figure 3 includes the

measurement uncertainty (the drop-to-drop statistical dispersion) of the measurements.

Although a vertical uplift is documented for point AG06, no monitoring of the field points BA01-09 is performed, e.g. by spirit leveling. Therefore, it is impossible to discriminate between the effects of a possible vertical uplift (as for point AG06) and the impact of (local) mass changes.
The continuous GNSS station PAOL is located between 300 and 500 m from the RG sites. The uplift measured at PAOL is due to regional tectonics, mostly governed by mountain building processes (Ching et al. 2011). Given the spatial wavelength of regional tectonics and since no active fault has been evidenced between PAOL and the RG sites, we can assume that both the AG and the RG sites experience the same uplift rate as recorded at PAOL. We updated lines 259-263.

- Ching, K.-E. E., Hsieh, M.-L. L., Johnson, K. M., Chen, K.-H. H., Rau, R.-J. J., & Yang, M. (2011). Modern vertical deformation rates and mountain building in Taiwan from precise leveling and continuous GPS observations, 2000-2008. J. Geophys. Res., 116(B8), B08406. https://doi.org/10.1029/2011JB008242

The relative gravity measurements were performed with only one relative gravimeter. For surveys in the microgal level, the control of the instrument is essential, both for the instrumental drift as well as for eventual steps due to transportation and handling and is usually realized by parallel observation with a second gravimeter.
We disagree with this comment as the use of “only one” relative gravimeter cannot be an argument to claim that resulting data are of poor quality. Actual fieldwork studies are done with a combination of one absolute and one relative gravimeter (Budetta et al. 1997; Carbone et al. 2003; Jacob et al., JGR 2010; Mouyen et al., GJI 2013; Pfeffer et al., WRR 2013), as we did. Measurements and processing were done applying all necessary steps (stabilization of the readings, re-measure of several sites, drift estimation, correction), all being described in lines 190-207 and comparable to those described in the studies cited above. Besides it is not usual to carry fieldwork measurements with two CG5, or any two relative gravimeters (Battaglia et al. 2008). Studies with two such devices are mostly meteorological works in controlled laboratory conditions (Jousset et al. 1995), and they are seldom.

- Battaglia, M., Gottsmann, J., Carbone, D., & Fernández, J. (2008). 4D volcano gravimetry. Geophysics, 73(06), WA3--WA18.
- Budetta, G., & Carbone, D. (1997). Potential application of the Scintrex CG-3M gravimeter for monitoring volcanic activity: results of field trials on Mt. Etna, Sicily. Journal of Volcanology and Geothermal Research, 76(3–4), 199–214. https://doi.org/10.1016/S0377-0273(96)00080-7
- Carbone, D. (2003). Bulk processes prior to the 2001 Mount Etna eruption, highlighted through microgravity studies. Journal of Geophysical Research, 108(B12). https://doi.org/10.1029/2003jb002542
- Jacob, T., Bayer, R., Chery, J., & Le Moigne, N. (2010). Time-lapse microgravity surveys reveal water storage heterogeneity of a karst aquifer. Journal of Geophysical Research, 115(B6), B06402. https://doi.org/10.1029/2009JB006616
- Jousset, P., Van Ruymbeke, M., Bonvalot, S., & Diament, M. (1995). Performance of two Scintrex CG3M instruments at the fourth International Comparison of Absolute Gravimeters. Metrologia, 32(3), 231–244. ttps://doi.org/10.1088/0026-1394/32/3/012

- Mouyen, M., Masson, F., Hwang, C., Cheng, C.-C., Le Moigne, N., Lee, C. W., … Hsieh, W.-C. (2013). Erosion effects assessed by repeated gravity measurements in southern Taiwan. Geophysical Journal International, 192(1), 113–136. https://doi.org/10.1093/gji/ggs019
- Pfeffer, J., Champollion, C., Favreau, G., Cappelaere, B., Hinderer, J., Boucher, M., … Robert, O. (2013). Evaluating surface and subsurface water storage variations at small time and space scales from relative gravity measurements in semiarid Niger. Water Resources Research, 49(6). https://doi.org/10.1002/wrcr.20235

The measurement scheme is not documented, only the reference to AG06 is mentioned. Textbooks on gravimetry document several schemes to control relative surveys which were not applied nor mentioned in the paper.
We now provide details about the relative gravity survey and processing in a new Appendix A. The only mandatory procedure is to repeat measurements at least at a base site (Reynolds, 2011), often being the site where AG is done for hybrid (AG+RG) microgravity surveys. We did it and also repeated measurements at several RG sites (lines 204-207).

- Reynolds, J. M. (2011). An introduction to applied and environmental geophysics. Wiley-Blackwell.

It is not true, that "Inferring this drift requires to regularly re-measure a base station where absolute gravity is known (AG06 in this case)" (L123). Drift and eventual steps can be analyzed and separated without any knowledge of the absolute gravity value, assumed a proper measurement scheme was chosen.
That is right. We remove “where absolute gravity is known”.

Further, a strict temporal regime is necessary to obtain reliable and reproducible measurements in the microgal range, which cannot be achieved by just observing the scatter of the readings. A variability of the observation time between 15 to 23 minutes (L121) will most likely include a change of the instrumental drift during movement and during rest, which degrades the obtained values systematically.
There is a misunderstanding here. We repeat measurements at each site until the gravity readings repeat within 3 microGal (line 193). That is our way to get reliable and reproducible results. We do not use the entire series of value measured over the 15-23 min but only the latter stable measurements. The drift is not computed over the 15-23 min but over the whole survey, merging all data from the repeated sites. This drift inversion is a standard procedure explained in Hwang et al (2002), cited on line 203. We rephrase this section (lines 204-207) to remove ambiguities on the drift adjustment.

Finally, the corrections due to ambient temperature variations are rather unusual and should be referred specifically to CG5#167, as documented in Fores et al. (2016).
The correction might be unusual, yet it is not an argument to dismiss it. The effect of temperature variations on gravity readings was already observed by several operators, including ourselves, yet informally. The Fores et al. (2017) is a dedicated meteorological study on this effect and it has been done with two CG5 (#167 and

#1151). Besides, we also used CG5#167 (line 614). We believe it is relevant to update processing workflow according to recent metrological studies.

The computation of the gravitational mass effects is not clear. While Figure 1 is showing a point mass approach, which is inadequate for the problem, later (L238) the prism approach of Nagy is mentioned. It should be clearly documented, which method the study is following.
This was indeed confusing. On one hand, we write on line 362: “rectangular prisms methods (Nagy, 1966)”. On the other hand, the point-mass approach is mentioned in the introduction (line 100), together with the new Figure 2 and equation 1. The aim of Figure 2 (ex Figure 1)/ Eq. 1 is to introduce time-variable gravimetry and its parameters in an easily understandable way to readers not familiar with this technique. We rewrite this paragraph more clearly and introduce the prism method as well already here to remove confusion (lines 100-126).

Although rectangular prisms are still widely used it should be checked whether more efficient and innovative methods, e.g. based on polyhedra, could be applied, see e.g. Petrovic(1996) or Tsoulis (2012) and references therein.
Indeed, other methods exist but the reason why we use rectangular prism for modelling gravity is that we constrain the gravity inversion by the changes of the ground surface, measured by photogrammetry. The photogrammetry data are provided as pixel maps, with a regular grid spacing of 50 cm (line 303). The best way to model gravity from the photogrammetry data is thus to use rectangular prisms, because such prisms can be set to fit exactly each pixel of the photogrammetry data. Arbitrarily shaped polyhedral modelling (Petrovic, 1996; Tsoulis, 2012) is indeed able to cope why irregular geometries but in our case, the best polyhedrons are rectangular prisms. As noted, prisms method remains a standard for dealing with gravity effects from surface topography (Torge & Müller, 2012, p.262).

- Torge, W., & Müller, J. (2012). Geodesy. Berlin, Boston: DE GRUYTER. https://doi.org/10.1515/9783110250008

The estimate of a density distribution lacks serious shortcomings. First, gravitational effects due to the landslide cannot be separated from changes in the sedimentation in the river bed. It is very likely that the documented gravity change between epochs 2015 and 2016 is caused mainly by the landslide, not by mass changes in the river bed. This is supported by the volume changes inferred from the photogrammetric approach. Therefore the estimate of a density distribution(!) by a least squares approach (which is basic and doesn’t need to be documented in a schematic way used for matrix computation) is highly unreliable.
We disagree with this comment. Indeed, it is possible to separate the density of landslide from the density of the river materials, because this a joint gravity-photogrammetry inversion, not just a gravity inversion. This is the interest of combining the gravity measurements with the photogrammetry measurement, as

well as the main novelty of this study. The inversion scheme is basic indeed but the design matrix A is not, because it is constructed thanks to the knowledge of the volume changes measured by photogrammetry (to our knowledge, no such joint photogrammetry-gravimetry survey has been done before). The problem can be solved for up to three different densities, which is nowhere referred to as a "density distribution" in the paper. These three densities (case 3, line 342 together with eq. 4) are the:

1. density of the landslide's materials
2. density of the sediments redistributed in the river between 2015 and 2016
3. density of the sediments redistributed in the river between 2016 and 2017

It is misleading to make an intuitive link (*"very likely that the documented gravity change between epochs 2015 and 2016 is caused mainly by the landslide"*) between the mass of sediment redistributed by the landslide and the gravity changes. Indeed, the distance between the redistributed mass and the gravity sites, which is to the power 2 (Eq. 1 line 102), will contribute significantly to the final gravity changes, yet our gravity sites are located next to the river and further from the landslide. We added also two subpanels in Figure 2 to emphasize the effect of the mass position on the gravity value.

Observation equations and correct uncertainty estimates are missing. Only the error of the a posteriori unit weight is given instead of the covariances of the estimated parameters (and their significance!). The ill-posed problem of the inversion of gravity changes with respect to mass variations is not sufficiently well addressed, see e.g. Prutkin and Casten (2009) and references therein.

Indeed, we used the a posteriori uncertainty of unit weight instead of the covariance matrix. We correct this error (lines 367-371, Table 3 and at any place where such values are mentioned).

The observation equation is given in eq. 2 (line 348). The uncertainties were detailed in lines 230-287 and Table 1 summarizes the uncertainties associated with each correction we applied on the data.

We understand the work of Prutkin and Casten (2009), indeed the ill-problem appears during the downward continuation step, since the potential field below the surface can't be constrained other than by surface gravity measurements. Yet we are not at all in this situation: we are interpreting gravity changes due to mass redistribution at the surface. Here we use photogrammetry data to constrain the geometry of the surface and fix the ill-posed problem. The paper cannot be fully understood by only focusing on the gravimetry.

The explanation of gravity changes due to vertical displacements (L150) is unacceptable. Not the distance to the "Earth's center of mass" is relevant, but the complex relation between the position of the sensor relative to the surrounding masses and their (re-)distribution.

Our explanation matches the standard understanding of the ground vertical displacement effect on the gravity changes (Van Camp et al, 2017). Free air effect is

defined as an effect of the change of the distance to the Earth's center of mass and is the most significant contribution to the effect of vertical displacement on gravity. The "*complex relation*" with the surroundings is the plateau effect. We do not reinvestigate this topic here and rather use a widely accepted value of -2 microgal/cm (line 259), as in others studies (De Linage et al., 2007; Mouyen et al., 2013; Van Camp et al., 2011).

- de Linage, C., Hinderer, J., & Rogister, Y. (2007). A search for the ratio between gravity variation and vertical displacement due to a surface load. Geophysical Journal International, 171(3), 986–994. https://doi.org/10.1111/j.1365-246X.2007.03613.x
- Mouyen, M., Masson, F., Hwang, C., Cheng, C.-C., Le Moigne, N., Lee, C. W., … Hsieh, W.-C. (2013). Erosion effects assessed by repeated gravity measurements in southern Taiwan. Geophysical Journal International, 192(1), 113–136. https://doi.org/10.1093/gji/ggs019
- Van Camp, M., de Viron, O., Scherneck, H.-G. G., Hinzen, K.-G. G., Williams, S. D. P., Lecocq, T., … Camelbeeck, T. (2011). Repeated absolute gravity measurements for monitoring slow intraplate vertical deformation in western Europe. Journal of Geophysical Research, 116(B8), B08402. https://doi.org/10.1029/2010JB008174
- Van Camp, M., de Viron, O., Watlet, A., Meurers, B., Francis, O., & Caudron, C. (2017). Geophysics From Terrestrial Time-Variable Gravity Measurements. Reviews of Geophysics, 55(4), 938–992. https://doi.org/10.1002/2017RG000566

Finally, the gravitational effect of the dolosses placed near to gravity site BA02 is unclear. Since the close proximity to the measurement point just a volume estimate as documented in Appendix A which is insufficient. Instead, an integration over the volume of these disturbing mass elements is necessary.
The integration over the volume is done thanks to the photogrammetry data and 3D-gravity modelling (Appendix B). We now emphasize this point more clearly in the text as well (lines 284-286).

In conclusion, the results of the gravimetric part of the study are neither based on a solid observational basis nor are they interpreted in a proper way. Therefore I cannot recommend the contribution in its present form for publication.
We hope that we have clarified the manuscript and answered the issues raised by the reviewer when appropriate.

References:

Petrovic S (1996) Determination of the potential of homogeneous polyhedral bodies using line integrals: Journal of Geodesy, 71, 44-52.
Tsoulis, D (2012) Analytical computation of the full gravity tensor of a homogeneous arbitrarily shaped polyhedral source using line integrals. Geophysics 77 (2): F1–F11.doi: https://doi.org/10.1190/geo2010-0334.1
I. Prutkin, U. Casten (2009) Efficient gravity data inversion for 3D topography of a contact surface with application to the Hellenic subduction zone, Computers & Geosciences, Volume 35, Issue 2

Revised manuscript with marks

Quantifying sediment mass redistribution from joint time-lapse gravimetry and photogrammetry surveys

Maxime Mouyen[1], Philippe Steer[2], Kuo-Jen Chang[3], Nicolas Le Moigne[4], Cheinway Hwang[5], Wen-Chi Hsieh[6], Louise Jeandet[2], Laurent Longuevergne[2], Ching-Chung Cheng[5], Jean-Paul Boy[7], Frédéric Masson[7].

[1]Department of Earth and Space Sciences, Chalmers University of Technology, Onsala Space Observatory, SE-439 92 Onsala, Sweden.
[2]Univ Rennes, CNRS, Géosciences Rennes, UMR 6118, 35000 Rennes, France.
[3]Department of Civil Engineering, National Taipei University of Technology, Taipei 10608, Taiwan, R.O.C.
[4]Géosciences Montpellier, UMR CNRS/UM2 5243, Université Montpellier 2, CNRS, Montpellier, France
[5]Department of Civil Engineering, National Chiao Tung University, Hsinchu 300, Taiwan, R.O.C.
[6]Industrial Technology Research Institute, Hsinchu 310, Taiwan, R.O.C.
[7]Institut de Physique du Globe de Strasbourg, CNRS - Université de Strasbourg UMR 7516 - Ecole et Observatoire des Sciences de la Terre, 67084 Strasbourg Cedex, France.

Correspondence to: Maxime Mouyen (maxime.mouyen@chalmers.se)

Abstract. The accurate quantification of sediment mass redistribution is central to the study of surface processes, yet it remains a challenging task. Here we test a new combination of terrestrial gravity and drone photogrammetry methods to quantify sediment mass redistribution over a 1-km^2 area. Gravity and photogrammetry are complementary methods. Indeed, gravity changes are sensitive to mass changes and to their location. Thus, by using photogrammetry data to constrain this location, the sediment mass can be properly estimated from the gravity data. We carried out 3 joint gravity-photogrammetry surveys, once a year in 2015, 2016 and 2017 over a 1-km^2 area in southern Taiwan featuring both a wide meander of the Laonong River and a slow landslide. We first removed the gravity changes from non-sediment effects, such as tides, groundwater, surface displacements and air pressure variations. Then, we inverted the density of the sediment, with an attempt to distinguish the density of the landslide from the density of the river sediments. We eventually estimate an average loss of $3.7 \pm 0.4 \times 10^9$ kg of sediment from 2015 to 2017, mostly due to the slow landslide. Although the gravity devices used in this study are expensive and need week-long surveys, new instrumentation progresses shall enable dense and continuous measurements at lower cost, making this method relevant to improve the estimation of erosion, sediment transfer and deposition in landscapes.

Deleted: 4

1 Introduction

The reliable quantification of sediment mass redistribution is critical to the understanding of surface processes (Dadson et al., 2003; Hovius et al., 2011; Morera et al., 2017) and has significant implications for studies in tectonics (Molnar et al., 2007; Steer et al., 2014; Willett, 1999), climate (Peizhen et al., 2001; Steer et al., 2012), human activities (Horton et al.,

2017; Torres et al., 2017) or biochemistry (Darby et al., 2016). The earth's topography is constantly eroded but the rates of this erosion vary whether they are estimated at decadal, thousand- or million-years timescales. Estimating such erosion rates over all these timescales provides a more complete description of their controlling processes (Dadson et al., 2003). These processes can run over millions to thousands years, such as tectonic uplift, in which case fission track thermochronometry (Fuller et al., 2006), cosmogenic nuclides (von Blanckenburg, 2006) or river terrace incision measurements (Hartshorn et al., 2002) are appropriate methods for estimating erosion rates. Nevertheless, rapid events such as earthquakes and landslides, very common in Taiwan, also play a significant role in eroding landscapes (Dadson et al., 2003; Hovius et al., 2000, 2011). At daily to decadal timescales, erosion is classically estimated from the concentration of the suspended sediment in the rivers draining the studied areas (Fuller et al., 2003; Milliman & Farnsworth, 2011; Walling & Fang, 2003). A significant proportion of sediment can also be transported on the river bed (Blizard & Wohl, 1998), that is bedload sediment transport, which automatic gauging stations do not measure, likely resulting in an underestimation of the erosion rate. Nevertheless, sediment inputs to rivers in areas prone to landslides are not immediately flushed to the ocean. They are rather evacuated over decadal timescales (Croissant et al., 2017; Hovius et al., 2011), generating large sediment mass redistributions, mixing suspended and bedload sediment transport, all along the rivers. Thus, this sediment mass redistribution should be quantifiable even with discontinuous observations.

Earth surface processes studies, either from models or field observations, rely on mass information. Indeed, the basis of surface process models is the mass conservation equation of sediment and in-situ sediment-transport lexical and variables, e.g. entrainment, sediment load or sediment delivery, also refer to sediment mass (Aksoy & Kavvas, 2005; Ferro & Porto, 2000; Milliman & Farnsworth, 2011). The development of optical methods, such as light detection and ranging (LIDAR) and photogrammetry, now allows to accurately measure ground surface elevation, leading to reliable estimations of rock or sediment volume redistribution between two instants (Jaboyedoff et al., 2012). However, these promising methods do not offer a direct estimate of mass changes and require relying on generally poorly known local values of the bulk density of sediments or rocks. In contrast to topographic measurement, gravity is an integrative measure, sensing all mass changes around the measurement site. However, gravimetry does not offer good constraints on the localisation of mass changes or on its volumetric extent. Therefore, we develop here a new approach, combining photogrammetry and terrestrial time-lapse gravimetry to estimate average sediment densities over the investigated area and to convert the volume of redistributed sediment into mass. This approach returns a density that automatically averages all sediment density heterogeneities of the area without the need of dense in-situ density measurements.

In this study, we quantify the sediment mass redistribution over an area of ~1 km^2 in southern Taiwan (Fig. 1), between 2015 and 2017. It aims at complementing suspended sediment measurements to better assess sediment mass redistribution at decadal timescales. The studied area hosts both a slow landslide and a river carrying sediments eroded from the inner part of the mountainous catchment.

Deleted: to

Deleted: such a

Deleted: ,

Deleted:

Deleted: ·

Deleted: The surveys were done once a year in 2015, 2016 and 2017.

Time-lapse gravimetry, that is the measure of gravity changes with time at a fixed location, is the only geophysical tool directly sensitive to mass redistributions at and below the earth's surface. It has been widely applied in the fields of glaciology, hydrology and solid earth processes, either from space, with the Gravity Recovery and Climate Experiment (GRACE) mission (Farinotti et al., 2015; Han et al., 2006; Longuevergne et al., 2013; Pail et al., 2015; Tapley et al., 2004), or from terrestrial instruments (Van Camp et al., 2017; Crossley et al., 2013). Recent studies demonstrate the new potential of time-lapse gravity for studying surface processes as well, because the mass of deposited or eroded sediment can also significantly alter the gravity field (Y.-C. Liu et al., 2016; Mouyen et al., 2013, 2018). Since gravimetry is presently undergoing a revival thanks to recent technological progresses (Ménoret et al., 2018; Middlemiss et al., 2016, 2017), new ranges of applications such as sediment mass quantification shall be encouraged to promote the use of gravimetry outside the field of geodesy.

The classical limitation for gravimetry is the non-uniqueness of its solutions, since gravity changes are integrative and sensitive to both mass variations and to the location where these mass variations take place (Fig. 2 and equation 1). Nevertheless, network gravity surveys have showed their high value to estimate below ground mass changes in hydrology (Jacob et al., 2010; Naujoks et al., 2008), volcanology (Carbone & Greco, 2007; Kazama et al., 2015) or reservoir monitoring evolution (Ferguson et al., 2008; Hare et al., 2008). When studying underground processes, especially groundwater, it is common to simplify the redistribution to a one-dimension problem. The groundwater level variations Δh are the main observable and gravity effects are computed using a Bouguer plate ($2\pi G \rho_{water} \Delta h$). This simplification is necessary because it is usually impossible to monitor lateral groundwater redistribution, yet it remains appropriate for homogeneous aquifers. The groundwater level variation can be assumed constant over the entire aquifer. Such an assumption is not valid for surface processes because sediment build complex three-dimensional bodies. But sediment mass redistributions occur at the ground's surface thus, they are accessible to accurate location methods such as photogrammetry (Eltner et al., 2016; Niethammer et al., 2012; Schwab et al., 2008). Combining accurate geometries with gravity variations must thus enable proper mass estimations. Fig. 2 illustrates the use of time-variable gravimetry to quantify sediment mass redistribution at the earth's surface. In the simplest case, when considering each ground element as a point-mass, the total change of gravity Δg measured between t_0 and t_1 is:

$$\Delta g = g_{t1} - g_{t0} = \sum_{i=1}^{N} \Delta g_i = \sum_{i=1}^{N} \frac{G m_i}{r_i^2} sin\theta \qquad (1)$$

where Δg_i is the vertical component of the gravitational change at each element i (i ranging from 1 to N = 28 in Fig. 2b) considered as a point-mass (Fig. 2c) of mass m_i located at a distance r_i from the gravimeter, and G is the universal gravitational constant. Note that the gravitational attraction of any element decreases with the square of the distance between this element and the site where gravity is measured, so that the distance of the mass redistribution can be a strong limiting factor to measure significant gravity changes. Note also how the angle θ between the point mass and the site where gravity is

Formatted: English (United Kingdom)

Deleted: (Ménoret et al., 2018; Middlemiss et al., 2017, 2016)

Deleted: ¶

Deleted: this method

Deleted: 1

Deleted: Unlike deep mass changes

Deleted: ,

Deleted: and

Deleted: therefore

Deleted: 1

Deleted: T

Deleted: 1b

Deleted: 1

measured contributes to the gravity effect. The gravity effect is maximum when the point mass is at the vertical of the site, negative if above the site, positive if below. If the point mass is exactly at the horizontal with the gravimeter sensor, then the gravity effect cancels. The effects of the angle and the distance are shown in Fig. 2d and 2e, for a general case and for one actual site of the survey, respectively. Point-mass simplification is ideal to grasp the concept of gravimetry survey, but is it not suitable for precise quantifications aimed to in this study. All gravity modelling will thus be done using rectangular prism modelling (Nagy, 1966), which is the most appropriate way to compute the gravity effect of surface changes measured by photogrammetry.

After introducing the study area, we describe the gravimetry and photogrammetry surveys that we conducted, together with our data processing workflow. We then show the results of both methods and interpret them jointly in order to retrieve the mass of sediment redistributed in this area from 2015 to 2017. We eventually discuss the benefits and limits of this method.

2 Study area

The joined gravimetry-photogrammetry survey was set in southern Taiwan, at the Paolai village, next to the Laonong River (Fig. 1). The gravity network contains one site, AG06, for absolute gravity (AG) measurement and nine sites, BA01 to BA09, for relative gravity (RG) measurements. During the 2017 survey, all sites but BA02 were located to cm accuracy using Global Navigation Satellite System (GNSS) enhanced by real-time kinematic (RTK) technique. The exact location of BA02 could not be measured due to the unexpected storage of concrete blocks, referred to as dolosse, aiming at being placed on the river shore to protect it from erosion. This dolosse storage also covered BA03 and BA04 but those two sites could still be measured. The gravimetric effect of the dolosse was estimated and removed from the measurements.

The first reason for choosing this location is that time-lapse absolute gravity surveys have been done at AG06 since 2006, in the frame of the Absolute Gravity in the Taiwan Orogen (AGTO) project. This project permitted to measure, for the first time, sediment mass redistribution using time-lapse absolute gravimetry and shown that significant sediment transfers occurred around Paolai (Kao et al., 2017; Mouyen et al., 2013). Indeed, this site experiences vigorous sediment transfer processes powered by heavy rains brought by tropical cyclones (typhoons) and monsoonal events, especially in May to August (Chen & Chen, 2003). The heavy rains destabilize the slopes of the Taiwanese high mountains, triggering landslides and debris flows (Chiang & Chang, 2011). This occurs on a regular basis: 5 to 6 typhoons make landfall in Taiwan every year (Tu et al., 2009), mostly between May and September. The most remarkable event was the 2009 Morakot typhoon, which produced the worst flooding in the last 60 years in Taiwan and up to 2777 mm of accumulated rainfall (Ge et al., 2010) and triggered 22 705 landslides with a total area of 274 km^2 (C.-W. Lin et al., 2011). Landsliding, which can also be triggered by regional active tectonics, is the main process supplying sediment to rivers in Taiwan (Dadson et al., 2003; Hovius et al., 2000).

Deleted:
Deleted: fictitious
Deleted: ¶
Deleted: Testing the combination of photogrammetry and gravimetry for monitoring surface processes is a valuable effort regarding the recent and ongoing progress in gravimetry
Field Code Changed
Deleted: ¶
Deleted: 2
Deleted: , although those
Deleted: reached since these blocks are not plain
Deleted: ir
Deleted: will be
Deleted: identify

The second reason for choosing this location is practical. Indeed, this location offers a stabilized path made of concrete on the southern bank of the Laonong River, where the relative gravity benchmarks could be properly set, on stable and sustainable sites, and easily accessed for measurements. Also, a continuous GNSS station, PAOL (latitude: 23.10862°, longitude: 120.70287°, elevation: 431 m), is co-located with the AG06 pillar and is maintained by the Institute of Earth Sciences-Academia Sinica (IES-AS, 2015). This permits to precisely take into account gravity changes only due to ground vertical displacements.

In this area, both the Laonong River and the landslide (Fig. 1) are susceptible to sediment transfers. The gravimetry-photogrammetry survey is setup to focus on these processes. Note that what we call the river (plain black line contour in Fig. 1) is the active channel bed that includes emerged alluviums. During yearly measurements, the water extent of the river only covers a fraction of this area, even if the period 2015-2017 has seen some higher water level and larger extents, especially during large floods.

Deleted: 2

Deleted: 2

3 Methods

This section introduces the two main methods used in this study: gravimetry and photogrammetry. Gravimetry is sensitive to masses and their distribution, while photogrammetry is here a geometric measure of the ground surface, hence of the sediment distribution. Therefore, combining gravimetry and photogrammetry removes the geometric ambiguity inherent to gravity measurements and allows to focus on sediment masses. This combination is done through a least-squares inversion to determine sediment density, that is a mass per unit of volume.

3.1 Time variable gravimetry

Gravity was measured at 10 sites (Fig. 1) in 2015, 2016 and 2017, always over two days in November, since the climatic conditions during this month are usually suitable for gravimetry fieldwork (e.g. no typhoon nor heavy rains, reasonable temperatures). By measuring gravity during the same period of the year, we also expect to minimize hydrological effects, which have an strong annual periodicity in this area (Chen & Chen, 2003). Absolute and relative gravity surveys were done in parallel, the same days.

Deleted: 2

Deleted: November

Deleted: as

Deleted: during this month

Relative gravity measurements were done using a Scintrex CG5 Autograv (serial number 167). The measurement principle is to assess length variations of a spring holding a proof mass between different times and places, using a capacitive displacement transducer, and convert them into gravity variations (Scintrex Ltd., 2010). The instrument is levelled at each site and repeats 90-seconds measurements continuously. We stop measurements when gravity readings repeat within 3 µGal (1 µGal = 10^{-8} m s^{-2}), while the internal sensor temperature remains stable. This usually takes 10 to 15 measurements, that is 15 to 23 minutes, although up to 25 measurements were required in some rare cases. Only the latest measurements, when

gravity readings are stable, are used in the gravity network adjustment, to estimate the drift estimat. Indeed, relative gravimeter measurements are subjected to an instrumental drift, which is corrected using the software Gravnet (Hwang et al., 2002). Inferring this drift requires to re-measure one or more sites within a few hours. In this study, all surveys start and end at AG06, which is also re-visited up to four times during the survey, together with other relative gravity sites (Appendix A). In addition, ambient temperature alters gravity measurements at a rate of -0.5 Gal $°C^{-1}$ (Fores et al., 2017). This effect was taken into account before adjusting the instrumental drift of the gravimeter.

The absolute gravity measurements were done using a Micro-g FG5 (serial number 224), which monitors the drop of a free-falling corner-cube in a vacuum. During its free fall, the positions and times of the corner-cube are precisely assessed using laser interferometry and an atomic clock (Niebauer, 2015; Niebauer et al., 1995). One measurement takes ~12 hours and consists in 24 sets of 100 test mass drops started every 30 min (one drop every 10 s). Measurements are always done overnight, when anthropogenic seismic noise and temperature variations are lower than during day time. A laser problem in the FG5 prevented us from measuring absolute gravity in 2017. This is compromising since the measurements at BA01-BA09 can only be interpreted relative to an absolute reference. A first option would be to disregard the gravity data measured in 2017 and not interpret the relative gravity changes between 2016 and 2017. This is a rather drastic solution and we prefer to use a likely gravity value for AG06 in 2017, keeping in mind that we may thus introduce an unknown but constant offset in the whole relative gravity data. We decide to estimate the AG06 absolute gravity value in 2017 as the mean of the values measured in 2014, 2015 and 2016, that is 978 713 845.1 ± 3 µGal (Fig. 3). We arbitrarily set the standard deviation to a value larger than usual at this site. In this case, the AG06 values in 2016 and 2017 are quite similar, less than 0.5 µGal difference. Although absolute gravity measurements at AG06 started in 2006 and repeated once a year except from 2011 to 2013, it is not possible to use these older data for the estimation of the 2017 value. Indeed, in 2009, typhoon Morakot and its subsequent massive landslides reset the whole area. The gravity offset between November 2008 and November 2009, i.e. before and after Morakot, is about 30 microGal and is due to large sediment redistribution in this area (Mouyen et al., 2013). Sediment redistribution due to Morakot was such an exceptional event, with a significant impact on gravity, that it must not be included in the extrapolation of the 2017 gravity value. The measurements from 2009-2010 were not used either because too much reconstruction work was ongoing at that time, taking out debris from the river, thus interfering with natural sediment redistribution.

To focus on sediment mass redistribution, other sources responsible for gravity changes must be removed from the gravity time series. Here, these effects are the tides, air pressure variations, polar motions, vertical ground motions and hydrology. These corrections are detailed in the next paragraph and summarized in Table 1.

Solid earth tides are computed using TSOFT (Van Camp & Vauterin, 2005) using tidal parameters from Dehant *et al.* (1999), referred to as WDD. Ocean tide loading effects are computed using the FES2004 model (Letellier et al., 2004) with the Ocean Tide Loading provider (Bos & Scherneck, 2003). Polar motions effects are computed using the International Earth

Deleted: with the

Deleted: R

Deleted: regularly

Deleted:

Deleted: a base station where absolute gravity is known

Deleted: (AG06 in this case) and at least to start and finish the survey at this base station.

Deleted: The absolute gravity value at AG06 was measured in 2014, 2015 and 2016 (Fig. 3) and we extrapolate the 2017 value as being the average of the three previous AG values, that is 978 713 845.1 ± 3 µGal.

Deleted: ¶

Rotation and Reference System Services parameters and the Absolute Observations Data Processing Standards (Boedecker, 1991). Atmospheric effects, that is gravity changes due to air masses, are corrected using local barometric records done at a continuous weather station located ~12 km west of Paolai (station C0V250) and an admittance factor of -0.3 µGal hPa^{-1} (Merriam, 1992). Solid Earth tides, ocean tide loading and atmosphere loading are corrected before the drift adjustment of the relative gravity measurements, because they can have significant effects over a few hours, that is while the relative gravity survey is done. Not correcting them would bias the drift estimation by mixing gravity changes due to the instrumental drift with those due to tides and atmosphere. Vertical displacements of the ground also change the gravity, because the gravity measured at any place on the Earth's surface depends on the inverse of the square of the distance between this site and the Earth's center of mass. Therefore, if the site is uplifting (further from center of mass) or subsiding (closer to the center of mass), it will have a lower or higher gravity value, respectively. This effect is corrected using continuous GNSS time series recorded at AG06 (the GNSS site PAOL is co-located to AG06, Fig. 4) and assuming a theoretical ratio $\Delta g/\Delta z$ = -2 µGal/cm (Van Camp et al., 2011), where Δg is the gravity change and Δz is the elevation change, at the same location. Between 2015 and 2017, the ground uplift at AG06 is about 1.3 cm yr^{-1}. That is a large uplift rate, explained by the active mountain building processes at work in Taiwan, where up to 1.9 $cm.yr^{-1}$ uplift is measured (Ching et al., 2011). Although the relative gravity sites are between 300 and 500 m from the PAOL permanent GNSS, we apply the same uplift correction to these sites as to AG06. Indeed, tectonic uplift is a regional feature and can be assumed constant over a few hundred meters, unless an active fault or more cross the area. But there is no evidence for such a fault in Paolai.

We also correct the effect of hydrology, which deforms the earth surface at the global scale and changes the groundwater mass attraction at local scales, near the gravimeter. This correction relies on global hydrological models. We consider two of them in this study:

1. the Global Land Data Assimilation System Version 2 (GLDAS-2) forcing the Noah land surface model (Rodell et al., 2004) and
2. the Modern-Era Retrospective Analysis for Research and Applications, version 2 (MERRA-2, Gelaro et al., 2017).

The gravitational effect due to each of these models is provided by the EOST loading service (Boy, 2015; Petrov & Boy, 2004). Unlike the other corrections, the hydrological correction may suffer large uncertainties because of (1) the complexity of hydrological processes, (2) the difficulty to measure groundwater and (3) its large effect on gravity (Jacob et al., 2009; Longuevergne et al., 2009; Pfeffer et al., 2013). Indeed, the effect of GLDAS-2 and MERRA-2 on gravity predict up to 20 µGal of seasonal amplitude in the hydrological signal, with sometimes large differences, up to 10 µGal, between the different models (Fig. 5). Nevertheless, surveying in November appears as a valuable way to decrease the hydrological impact on the gravity data, since this effect is lower than 3 µGal, with any of the two hydrological models. Eventually we use the average hydrological effect from GLADS-2 and MERRA-2. We arbitrarily set an uncertainty of 5 µGal to this correction (Table 1), to account for possible bias in the models.

Deleted: ¶

We also correct the effect of the dolosse set in 2017, which is only significant at BA03 and BA04. These structures, located above BA03 and BA04, were indeed responsible for an artificial decrease of gravity of about 15 µGal. Their gravitational effect is computed using the dolosse's geometry measured by the photogrammetry and rectangular prism method (computation details in Appendix B). Given the uncertainty of this correction process, we add an arbitrary 5 µGal uncertainty on the gravity changes measured at BA03 and BA04 during the 2017 survey.

Deleted: Note that w

Deleted: A

3.2 Photogrammetry

An Unmanned Aerial Vehicle (UAV), commonly known as a drone, is an aircraft without human pilot on board and has been used in many disciplines, especially in morphotectonic studies (Chang et al., 2018; B Deffontaines et al., 2018; Benoît Deffontaines et al., 2017). To generate a high-resolution digital surface model (DSM), orthorectified mosaic images, and a true 3D model, the UAV mounted with a Sony ILCE-QX1 camera and a 16 mm SEL16F2.8 lens was used in this study (Fig. 6). The UAV is a modified already-available Skywalker X8 fixed-wing aircraft reinforced by carbon fiber rods and Kevlar fiber sheets. Launched by hand, it flies, takes photos, and lands autonomously by using a pre-programmed flight plan. The autopilot system is composed and modified from the open source APM (Ardupilot Mega 2.6 autopilot) firmware and open source software Mission Planner, transmitted by ground-air XBee radio telemetry.

The flight missions were planned with 300-500 m mean above ground level, covered an area of about 15-20 km^2 with about 10-15 cm ground sampling distance (GSD) in one single flight mission. Repeated adjacent photographs were kept for at least 85 % endlap and 50 % sidelap. Each UAV flight missions took about 90 min. The data sets, including orthomosaic images, DSM, and true 3D model, were generated and processed using ContextCapture and Pix4Dmapper with a grid spacing of 50 cm. 21 ground control points and 11 check points were measured in the field to control and to verify the quality of the datasets (Fig. 6c).

Deleted:

4 Survey results

The results of the gravity and photogrammetric surveys are summarized in Figs. 7 and Table 2. The largest gravity changes occurred between 2015 and 2016, with most sites showing an increase of more than 30 µGal. On the contrary, the gravity decreased at most sites from 2016 to 2017. When measured above the redistributed masses, increase and decrease of gravity correspond to gain and loss of masses, respectively. Qualitatively, this is in agreement with the corresponding digital surface models (DSM) changes in the active bed channel showing higher sediment thicknesses, thus a gain of mass, from 2015 to 2016 and large surfaces of lower sediment thicknesses from 2016 to 2017. Over the time period 2015-2016, the top of the landslide is actively eroded, up to 46 m, while its toe displays significant sedimentation, up to 33 m. The active river bed shows a mixed-pattern of erosion and sedimentation, between -1.19 and 1.21 m on average, possibly resulting from the

Deleted: shown

Deleted: 8, respectively

migration of the river braids. Whereas, over the time period 2016-2017, the landslide displays mostly erosion, up to 39 m, while the river bed continues to display a mixed-pattern of erosion and sedimentation, between -1.17 and 1.08 m on average.

The gravimetric and photogrammetric techniques show large changes in gravity and topography, which demonstrate active processes of sediment mass redistribution in the river and on the slow landslide. In the next section, we combine these results to assess the mass of sediment redistributed from 2015 to 2017. Note that we focus the DSM analysis to the area bounded by the black line in Figs. 7d and 7e, which is restricted to the landsliding zone and the river.

Deleted: 8

Deleted: 8

5 Joint analyses of the gravity and photogrammetry data

Using the DSM, we build rectangular prisms with horizontal sides of 0.5 m, i.e. DSM resolution, and a vertical side as high as the elevation at the time of the corresponding surveys, i.e. bottom at 0 m and top at the surface elevation. Among the three (2015, 2016 and 2107) photogrammetric surveys, the 2017 survey has the smallest surface extent. Its limits are thus used to cut the 2015 and 2016 photogrammetric surveyed areas, so that all DSM cover the exact same area. The total mass of redistributed sediment equals the change of volume between each survey multiplied by the density of the sediment. We use the gravity data to assess this density using an inverse modelling approach. Note that since gravity decreases with the square of the distance between the measurement site and the mass location, we can bound our analysis to the area covered by the photogrammetric surveys without biasing the analysis. Indeed, using the wider 2015 and 2016 survey coverages, we find that extending our working area in the north-south and east-west directions by steps of 100 m does not alter the gravity changes computed at each sites by more than 1 %.

We design three inversion cases to retrieve the densities of the redistributed materials, using a least-square criterion. These cases are independent from each other and aim at increasing the amount of possibly different densities for comparison. Thus we invert:

- Case 1: The average density ρ of the material redistributed during the surveys.
- Case 2: The density of the sediment in the river ρ_r and the density ρ_l of the material in the landslide.
- Case 3: The density of the sediment in the river ρ_r^{1615} from 2015 to 2016 and ρ_r^{1716} from 2016 to 2017 and the density ρ_l of the material in the landslide.

Here we will solve an over-determined problem, where we have more observations (20 gravity differences over the three years) than variables to estimate (density, three at most, in case 3). However, gravity observations are too few and unevenly distributed over the study area to try to invert the density at each pixel (more than 4 millions) of the photogrammetry survey. In practice, the matrix representation of this system is (e.g. Hwang et al., 2002)

$$L + V = AX \quad (2)$$

where the design matrix **A**, vector of unknowns **X** and vector of observations **L** are defined as

$$A = \begin{bmatrix} dg_{mod,r}^{1615,BA01} & 0 & dg_{mod,l}^{1615,BA01} \\ \vdots & \vdots & \vdots \\ dg_{mod,r}^{1615,AG06} & 0 & dg_{mod,l}^{1615,AG06} \\ 0 & dg_{mod,r}^{1716,BA01} & dg_{mod,l}^{1716,BA01} \\ \vdots & \vdots & \vdots \\ 0 & dg_{mod,r}^{1716,AG06} & dg_{mod,l}^{1716,AG06} \end{bmatrix} \quad (3)$$

$$X = \begin{bmatrix} \rho_r^{1615} \\ \rho_r^{1716} \\ \rho_l \end{bmatrix} \quad (4)$$

$$L = \begin{bmatrix} dg_{obs}^{1615,BA01} \\ \vdots \\ dg_{obs}^{1615,AG06} \\ dg_{obs}^{1716,BA01} \\ \vdots \\ dg_{obs}^{1716,AG06} \end{bmatrix} \quad (5)$$

and **V** is the vector of residuals (**X** and **V** are to be determined by the least-squares method). In matrices **A** and **L**, dg is the gravity variation that is modelled (dg_{mod}) or observed (dg_{obs}) between 2016 and 2015 (1615) or between 2017 and 2016 (1716) at every site (BA01… AG06). The modelled gravity change can be computed for the material in river ($dg_{mod,r}$) or in the landsliding zone ($dg_{mod,l}$). This matrix representation is given for the inversion case 3 and can be simplified for cases 1 and 2.

The design matrix **A** is built thanks to the photogrammetry surveys, from which we identify the river and the landslides as well as their respective volume changes. Therefore, knowing also the position of the gravity sites, we compute each element of **A** using a gravity modelling by rectangular prisms methods (Nagy, 1966) and an arbitrary density equal to 1. The actual density can be inverted by

$$X = (A^T PA)^{-1}(A^T PL) \quad (6)$$

where $\mathbf{A}^{\mathrm{T}}$ is the transpose of **A**. The weight matrix **P** is diagonal, and its elements are the invert of the gravity uncertainties at each site i. The residuals $V = AX - L$ are used to compute a posteriori variance of the unit weight

$$\sigma_0^2 = V^T PV/(n-u) \quad (7)$$

where n is the number of gravity observations and u the number of unknown densities and eventually the uncertainties of the inverted densities are the square root of the diagonal element of the a posteriori covariance matrix of **X**.

$$C_X = \sigma_0^2 (A^T PA)^{-1} \quad (8)$$

The inverted densities for each case are summarized in Table 3. Cases 1 and 2 return similar densities. Case 3 returns a noticeable difference between the densities of the sediment in the active bed channel for the 2015/2016 or 2016/2017 surveys. A first hypothesis for this difference could be that the composition of the redistributed sediment has changed over

Deleted: PAOL

Deleted: 3D

Deleted: Finally, t

Deleted: the uncertainty of the inverted densities as

Deleted: .

Deleted: 2

the years of the study, for instance because they come from landslides that occurred in terrain with different densities. A second hypothesis is that the water content of the sediment varies, eventually changing the effective density of the sediment as measured by the gravimeters. We do not have enough data to favor one of these hypothesis but we will discuss the possible influence of water on our density estimates in section 6.1. Uncertainties on the landsliding materials densities (case 2 and 3) are higher than those of the river sediment, likely because they are further from the gravity sites than the river sediment. As seen in equation 1, the further the redistributed masses are, the lower are their gravitational effects.

For comparison, during the 2017 survey, we evaluate the in situ densities of the materials in the active river bed and at the bottom of the landslide, at 22 sites (Fig. 8), also using photogrammetry (Appendix C). Estimating in situ density is time-consuming and demanding. It is done here only for comparison purposes; it is not required for the inversion. Indeed, joint gravity-photogrammetry estimates an average in situ density over the surveyed area. Besides, in situ density measurements are done at discrete locations over an area made of heterogeneous material. The in situ densities range from 1.2 to 2.7×10^3 kg m^{-3} and are spatially heterogeneous, illustrating the variety of materials carried by the river and the landslide. Despite the limited and spatially uneven sampling points, we obtain an average density (2.0×10^3 kg m^{-3}) consistent with the average densities inverted from the gravity and photogrammetry data (1.9×10^3 kg m^{-3}).

The final comparison of the measured gravity and the computed gravity in cases 1, 2 and 3 is given in Fig. 9. The largest misfits are at BA05 and BA06 during the 2016-2017 period, for which gravity changes are underestimated by 19 and 15 µGal, respectively. Possible explanations for these two misfits are: a wrong site location, an error in the gravity data, an error in the DSM data or local but large hydrological effects, not accessible at the scale of the global hydrological models we used. However, we could not narrow our search down a specific issue at BA05 and BA06. At the other sites, the pattern and amplitude of the gravity observations is rather well explained by the modelling. Note that in Fig. 9b, the gravity modelled at most sites seems to need a small offset of -3 µGals to fit within the error bars of the observations. This may show that our absolute gravity estimate for the 2017 survey (Fig. 3) is wrong by 3 µGals.

Multiplying the inverted densities (Table 3) with the volumes changes computed from the DSM changes, we can eventually compute the mass of sediment that were redistributed between two surveys, for each inversion cases (Fig. 10). Since the inverted densities are similar in each case (Table 3) and the volumes changes estimated from photogrammetry are identical, thus the estimated masses (volumes times density) are also similar in each three case. The difference mostly lies within the uncertainty of these estimates. In our mass estimation, we also differentiate the top and the toe of the landslide, because the top of the landslide mostly experience erosion, while its toe undergoes both erosion and sedimentation processes. This helps to unravel how the sedimentation and erosion processes are distributed over the slow landslide.

Deleted: 's

Deleted: 9

Deleted: B

Deleted:

Deleted: purposes,

Deleted:

Deleted: 10

Deleted: or

Deleted: yet,

Deleted: , showing the interest of coupling gravity and photogrammetric surveys to retrieve the density of the redistributed materials

Deleted: 10

Deleted: 2

Deleted: 1

Deleted: three

Deleted: 2

In the river only, we observe that the mass of sediment redistributed between each survey is similar. The river gained between 0.61 and 0.83×10^9 kg and lost between 0.58 and 0.74×10^9 kg. Thus, the mass loss is about 4% and 12% less than the mass gain, resulting in a quasi-balanced budget that is within the uncertainty of the mass estimations. The time variability of the sediment mass budget is dominated by the landslide, which causes larger mass redistributions (up to 4×10^9 kg) and loss-to-gain ratios. A significant mass loss occurred between 2016 and 2017, which is ~15 times larger than the mass gain. Between 2015 and 2016, both erosion and sedimentation are significant at about 2 to 3×10^9 kg, which are rather balanced. A likely hypothesis is that we mainly observe a transfer of sediment from the top of the landslide, where 2.1 ± 0.4×10^9 kg of material were eroded toward its toe, where 1.9 ± 0.4×10^9 kg accumulated (average mass from the three cases). Overall, from 2015 to 2017, the area has lost about 3.7 ± 0.4×10^9 kg of sediment. Note that this landslide occurs over several years, not in one quick event, probably as the consequence of the erosion by the meandering Laonong River.

Deleted: 6

Deleted:

Deleted: to accumulate

Deleted: 5

Deleted: here

Deleted: 4

6 Discussion

6.1 Implications for sediment transfers in active landscapes

Our results highlight how landscapes react to landsliding and how they evolve after a large perturbation such as the 2009 Morakot typhoon. Between 2015 and 2016, the activity of the Paolai slow landslide mostly consists in transferring about 2×10^9 kg (about 1×10^6 m^3) of materials form the landslide top to the landslide toe over roughly 100 to 200 m. After 2016, a significant event of erosion of the landslide occurs, with more than 3×10^9 kg of sediment removed, including most of the sediment previously deposited on the landslide toe. This corresponds to a particularly rapid evacuation of the sediment, especially in the alluvial context of the Laonong river, that is yet consistent with predictions obtained with a morphodynamic model by Croissant et al. (2017) for bedrock rivers. It is likely that the position of the landslide in the outer bank of a meander has favored sediment export efficiency. Despite this landslide activity, it is quite remarkable that the Laonong river roughly maintains a neutral sediment budget over 2 years, between 2015 and 2017, in the vicinity of the landslide. This means that the river mainly acts as a sediment transfer zone and that river incision and sediment evacuation occurring along the river is balanced by the sediment delivery occurring by the supply of landslide materials. This sediment supply may originate from the several large landslides triggered in the Paolai area by the 2009 Morakot typhoon (C.-W. Lin et al., 2011) and the following massive sediment aggradation along fluvial valleys up to 10, 30 and even possibly 100 m (DeLisle & Yanites, 2018; Hsieh & Capart, 2013). Our results would thus suggest that the Laonong river has not yet recovered from this aggradation phase and that the landscape is still perturbed by the aftermath of Morakot typhoon, even 8 years after its occurrence. This exceeds the relaxation time of 6 years observed after the 1999 Chi-Chi earthquake using river suspended load (Hovius et al., 2011). But typhoon-triggered landslides occur every year in Taiwan, and global warming may intensify this process (Chiang & Chang, 2011). This could also build and maintain long-term sediment sources within the Taiwan range, which will keep supplying sediment into rivers even long after the Morakot-induced sources have been completely flushed.

6.2 Impact of river water storage changes

The mass of sediment redistributed in the studied area from 2015 to 2017 was computed by multiplying the volume of redistributed sediment by a density estimated from the joint analysis of gravity and photogrammetry data. We tested several ways of separating materials: active river bed or landslide materials and active river bed material between 2015 and 2016 or between 2016 and 2017. However, the active river bed also includes the actual Laonong River, that is water with density $\rho_w = 10^3$ kg m^{-3}. The photogrammetry actually measures the river surface but the volume of the river, made only of water, cannot be isolated from the active river bed because the bathymetry of the river is unknown. Consequently, without the river depth's geometry, we cannot turn the river into rectangular prisms for computing its gravity effect. As a workaround, here we simply assume a constant river depth of 1 m, which corresponds to very rough field estimates. Then, we map the surface limits of the river from the optical images taken by the UAV during each survey. The height h of the river surface is given by the photogrammetry results. The river is then divided into prisms covering the river area, with sides of 0.5 m, upper face at elevation h and lower face at elevation h-1, since the river is 1-m deep. We then compute the gravity effect of the river on each site of the network (except BA02, which position is unknown). This effect is removed from the gravity observation and the average density inversion (case 1) is run, giving $\rho = 1.7 \pm 0.1 \times 10^3$ kg m^{-3} and RMS = 9.7 µGal. This represents a decrease of 11% relative to the density $\rho = 1.9 \pm 0.1 \times 10^3$ kg m^{-3} given in Table 1 and also relative to the mass budget in Fig. 10. These values are yet to be taken with caution since we do not know the exact geometry of the river, its depth in particular.

Deleted: we did not make the distinction between the water and

Deleted: 3D

Deleted: Eventually, t

Deleted: 2

Deleted: 1

6.3 Perspectives from recent progresses in gravimetry

In this study we take advantage of the intense surface processes occurring in Taiwan to jointly analyze both time-variable gravity and photogrammetry measurements. Indeed, the amplitude of the sediment mass redistribution guarantees to measure significant gravity changes and, most importantly, surface elevation changes. Nevertheless, for rivers experiencing large and dynamic sediment mass redistributions that yet remain hidden beneath the water level, photogrammetric data would not bring any constraint on the density inversion. One should thus only rely on the gravity measurements, leading to non-uniqueness problem, since both the density and the location of the redistributed sediment would have to be inverted. To better deal with this issue, we suggest two improvements to our gravity survey:

1. Set a denser network of gravity sites, ideally with a mesh structure. Indeed, more measurements, evenly distributed, mean more constraints on the density inversion.
2. Set this network closer to the mass changes to increase the gravity signal. The best option would be to locate the gravimeters directly beneath the river bottom. Fig. 11 shows that for such gravimeters, the average gravity change would increase from 31 to 50 µGal between 2016 and 2015 and from 13 to 61 µGal between 2017 and 2016.

Deleted: -location

Deleted: 2

This survey implies that gravimeters are set permanently over the time-period of the project, as they won't be easily accessible. Such a setup of buried permanent gravimeters is presently impossible to realize with CG5 or any other

contemporary relative or absolute gravimeter, but remains realistic at a few-years timescale. Indeed, a new generation of relative gravimeters is rising from the use micro-electro-mechanical systems (MEMS) technology, characterized by a significantly smaller size and lower price (H. Liu & Pike, 2016; Middlemiss et al., 2016, 2017). Those shoebox-sized devices could be used to set permanent and dense gravity networks in areas experiencing vigorous sediment transport. Gravity changes densely sampled over the river will permit to retrieve the sediment mass redistribution using gravity inversion methods (e.g. Camacho et al., 2011) further constrained by the geometry of the river and the depth of the relative gravimeter. In addition, as relative gravimeters suffer from instrumental drift, this buried permanent network should be run in parallel to either permanent absolute measurements, which has recently become possible thanks to quantum gravimeters achieving 1 µGal repeatability (Ménoret et al., 2018), or to slowly drifting superconducting gravimeters (Hinderer et al., 2015). Therefore, ongoing progresses in the development of terrestrial gravimeters may open new opportunities for quantifying the mass of sediment redistributed by surface processes. Another interest for having such a permanent gravity network is to monitor the dynamics of the sediment mass redistribution at timescales shorter than one year, since the sediment concentration in Laonong river varies across the year (Fig. 12a).

Deleted: (both mass change and position)

Deleted: 3

6.4 Continuous sediment transport estimation

When sediment concentration is not continuously measured, sediment rating curves are a convenient workaround which permits, once determined, to estimate sediment transport from water discharge measurements only (Horowitz, 2003). Indeed, continuous water discharge is less complicated to measure than sediment concentration. But this method, which does not properly capture the bedload transported sediment, is inappropriate for landslide-dominated mountain belts such as Taiwan (Blizard & Wohl, 1998; Hovius et al., 2000). In addition, sediment rating curves experience temporal variation (Huang & Montgomery, 2013; Morera et al., 2017) and can also be altered by the release of groundwater (Andermann et al., 2012). Thus, the proper use of rating curves is bounded to specific conditions that are yet to be validated for the Laonong River. Here we discuss the use of gravity for estimating the total sediment discharge of the Laonong River, that is suspended and bedload sediment transport.

Deleted: measuring

The method and perspectives introduced so far aim at quantifying the mass of sediment redistributed by an event with large sediment transport ability, such as a landslide or a high river discharge. The time step of this quantification depends on how long these events take to redistribute the sediment in a way that significantly alter the gravity measured at each site by, e.g., >10 µGal, as an indicative change. Nevertheless, the best solution is to set a permanent gravity network, so that any rapid sediment mass redistribution can be recorded. Fig. 12a shows that the largest sediment concentration recorded at LiuGui station is 5000 ppm (mass fraction), when the river level increased by 1.6 m.

Deleted: Thus, t

Deleted: 3

For the hypothetical permanent buried gravity network (Fig. 11c), we compute the gravity effect of a river level change of 1.6 m, which covers the entire area of the active bed channel of Laonong River. The 5000-ppm sediment concentration

Deleted: 2

means there is 5 kg of sediment in 1000 kg of river's fluid, hence 995 kg of pure water. In this framework, and assuming that the density of the sediment is 2×10^3 kg m^{-3}, we can compute the density change due to rising sediment concentrations, until 10^6 ppm, meaning the river is made of sediment only. The gravity variation solely due to 5000 ppm of suspended sediment is about 0.17 µGal on average over each site. This cannot be properly distinguished from the main gravity change due to the rising river water level. Thus, time-variable gravity would not have been sensitive to the instantaneous suspended sediment concentration of the Laonong River between 2015 and 2017, even with a gravity network beneath the riverbed. In fact, the suspended sediment concentration would need to be about 3×10^5 ppm to change the gravity by at least 10 µGal (Fig. 12b with the bedload set to 0 cm). This corresponds to a concentrated debris-flow, nearly 8 times more concentrated than the threshold of 4×10^4 ppm used for debris-flow definition (Dadson et al., 2005; G.-W. Lin & Chen, 2013). However, sediment is also transported on the river bed, as bedload, and it must be added to suspended sediment concentration to make a complete estimation of the sediment discharge effect on gravity. We have no measurement of this bedload component for Laonong River but measurements in another catchment of Taiwan showed that 50% of the cumulative mass of the bedload was built by rocks which diameter is 15 cm (D_{50} = 150 mm) and D_{90} = 62.5 cm (Cook et al., 2013). Therefore, we compute the effect of homogenous bedload layers of up to 60 cm thickness and density 2×10^3 kg m^{-3} and add it to the suspended sediment effect (labelled curves in Fig. 12b). It generates about 50 µGal of gravity variation, which would be clearly identifiable in the gravity measurements. This computation gives an order of magnitude of the gravity change expected from time-varying suspended and bedload transport. It shows that continuous time-variable gravity could quantify sediment discharge if the sediment concentration is at least 3×10^5 ppm without bedload, or if the bedload is at least 12.5 cm thick, under the assumption that only gravity changes above 10 µGal are significant. More accurate prediction of gravity effects require to know the proportionality relation, if any, between the suspended and bedload component, as well as local hydrogravity models. Again, this 10-µGal threshold is linked to the accuracy of todays' gravimeter but ongoing progresses and interest in time-variable gravimetry may fuel the development of devices with higher accuracies.

Deleted: should

Deleted: 3

Deleted: strong

Deleted: 3

Deleted: s

Deleted: .

7 Conclusion

This study shows that the mass of sediment redistributed by rivers and landslides can be estimated by combining time-lapse gravimetric and photogrammetric measurements. Focusing on the Laonong River, in southern Taiwan, we estimate that about 3.7 ± 0.4×10^9 kg of sediment were removed from 2015 to 2017 around our study site. This sediment loss is mainly due to a slow landslide moving from one year to another. The sediment budget (i.e. the difference between sedimentation and erosion) within the river is close to zero, although more surveys should be carried out to identify longer-term deposition or erosion in this area. The average sediment density obtained with this method (1.9 ± 0.01×10^3 kg m^{-3}) is similar to the average sediment density measured in situ across the flood plain (2.0×10^3 kg m^{-3}). The new method introduced in this paper has the advantage to directly sense the mass of sediment, without using rating curves or in situ sediment concentration data. Therefore, it can benefit a wealth of studies on surface processes, which require quantitative estimates of sediment mass

Deleted: 4

Deleted: 2

Deleted: 2

redistribution. Although time-variable gravimetry remains a rather expensive method with demanding survey constraints, it has undergone promising progresses in the recent years. One is the significant miniaturization of the devices, using inexpensive MEMS technology (Middlemiss et al., 2016), the other is the realization of permanent absolute gravimeters, using cold-atom interferometry (Ménoret et al., 2018). Such new tools could be further used without photogrammetry, for rivers where most of the sediment transport is hidden under the water. If the suspended and bedload transport are significant enough, measuring the instantaneous sediment discharge could also become a reasonable project.

Data availability

All data are available in a public archive downloadable at this address:
https://chalmersuniversity.box.com/s/q5h1lpbflqlx9wi9yruway3k9jorflwe

Author contribution

P.S., M.M. and L.L conceived the study. M.M., N.L.M. and W.-C.H. acquired and processed the gravimetry data. K.-J.C. acquired and processed the photogrammetry data. L.J. and M.M. made the in situ sediment density measurements. C.H. acquired and processed the GPS-RTK data. J.-P.B. computed the hydrological loading effect on gravity. F.M initiated the AGTO project. M.M. performed the main analysis. All authors contributed to the final form of the article.

Competing interests:

The authors declare that they have no conflict of interest.

Acknowledgments

M.M. did the fieldwork and part of the analysis study while being a postdoctoral researcher at Geosciences Rennes, supported by a postdoctoral grant of the Centre National d'Etudes Spatiales (CNES) and by the CRITEX project funded by the Agence Nationale de la Recherche (ANR-11-EQPX-0011 and the Brittany region). We acknowledge support by the EROQUAKE project funded by the Agence Nationale de la Recherche (ANR-14-CE33-0005) and from the France-Taiwan International Associate Laboratory "From Deep Earth to Extreme Events" (LIA-D3E, http://www.lia-adept.org/). We are grateful to the RESIF-GMOB (http://www.resif.fr) facility for providing us with the relative gravimeter Scintrex CG5 #167. The authors acknowledge the Taiwan Typhoon and Flood Research Institute, National Applied Research Laboratories, for providing the Data Bank for Atmospheric & Hydrologic Research service. Figs 1, 7 and 9 were done with GMT (Wessel et al., 2013). We thank two anonymous reviewers, which comments improved the manuscript.

Formatted: Not Highlight
Deleted: Data are
Deleted: online
Formatted: Not Highlight
Formatted: Not Highlight
Deleted:
Field Code Changed
Deleted: from the corresponding author on reasonable request
Formatted: Not Highlight
Formatted: Not Highlight

References

Aksoy, H., & Kavvas, M. L. (2005). A review of hillslope and watershed scale erosion and sediment transport models. In *Catena* (Vol. 64, pp. 247–271). https://doi.org/10.1016/j.catena.2005.08.008

Andermann, C., Bonnet, S., Crave, A., Davy, P., Longuevergne, L., & Gloaguen, R. (2012). Sediment transfer and the hydrological cycle of Himalayan rivers in Nepal. *Comptes Rendus Geoscience*, *344*(11), 627–635. https://doi.org/https://doi.org/10.1016/j.crte.2012.10.009

von Blanckenburg, F. (2006). The control mechanisms of erosion and weathering at basin scale from cosmogenic nuclides in river sediment. *Earth and Planetary Science Letters*, *242*(3), 224–239. https://doi.org/https://doi.org/10.1016/j.epsl.2005.11.017

Blizard, C. R., & Wohl, E. E. (1998). Relationships between hydraulic variables and bedload transport in a subalpine channel, Colorado Rocky Mountains, U.S.A. *Geomorphology*, *22*(3), 359–371. https://doi.org/https://doi.org/10.1016/S0169-555X(97)00055-X

Boedecker, G. (1991). IAGBN: Absolute Observations Data Processing Standards. *BGI-Bull. d'Information*, *69*, 25.

Bos, M. S., & Scherneck, H.-G. (2003). Ocean tide loading provider. Retrieved from http://holt.oso.chalmers.se/loading/

Boy, J.-P. (2015). EOST Loading Service.

Camacho, A. G., Fernández, J., & Gottsmann, J. (2011). The 3-D gravity inversion package GROWTH2.0 and its application to Tenerife Island, Spain. *Computers & Geosciences*, *37*(4), 621–633. https://doi.org/10.1016/j.cageo.2010.12.003

Van Camp, M., & Vauterin, P. (2005). Tsoft: graphical and interactive software for the analysis of time series and Earth tides. *Comput. Geosci.*, *31*(5), 631–640. https://doi.org/10.1016/j.cageo.2004.11.015

Van Camp, M., Williams, S. D. P., & Francis, O. (2005). Uncertainty of absolute gravity measurements. *Journal of Geophysical Research*, *110*(B5), B05406. https://doi.org/10.1029/2004JB003497

Van Camp, M., de Viron, O., Scherneck, H.-G. G., Hinzen, K.-G. G., Williams, S. D. P., Lecocq, T., et al. (2011). Repeated absolute gravity measurements for monitoring slow intraplate vertical deformation in western Europe. *Journal of Geophysical Research*, *116*(B8), B08402. https://doi.org/10.1029/2010JB008174

Van Camp, M., de Viron, O., Watlet, A., Meurers, B., Francis, O., & Caudron, C. (2017). Geophysics from terrestrial time-variable gravity measurements. *Reviews of Geophysics*, *55*(4), 938–992. https://doi.org/10.1002/2017RG000566

Carbone, D., & Greco, F. (2007). Review of microgravity observations at Mt. Etna: a powerful tool to monitor and study active volcanoes. *Pure and Applied Geophysics*, *164*(4), 769–790. https://doi.org/10.1007/s00024-007-0194-7

Chang, K.-J., Chan, Y.-C., Chen, R.-F., & Hsieh, Y.-C. (2018). Geomorphological evolution of landslides near an active normal fault in northern Taiwan, as revealed by lidar and unmanned aircraft system data. *Nat. Hazards Earth Syst. Sci.*, *18*(3), 709–727. https://doi.org/10.5194/nhess-18-709-2018

Chen, C. S., & Chen, Y. L. (2003). The rainfall characteristics of Taiwan. *Monthly Weather Review*, *131*(7), 1323–1341.

Chiang, S. H., & Chang, K. T. (2011). The potential impact of climate change on typhoon-triggered landslides in Taiwan,

2010-2099. *Geomorphology*, *133*(3–4), 143–151. https://doi.org/10.1016/j.geomorph.2010.12.028

Ching, K.-E. E., Hsieh, M.-L. L., Johnson, K. M., Chen, K.-H. H., Rau, R.-J. J., & Yang, M. (2011). Modern vertical deformation rates and mountain building in Taiwan from precise leveling and continuous GPS observations, 2000-2008. *J. Geophys. Res.*, *116*(B8), B08406. https://doi.org/10.1029/2011JB008242

Cook, K. L., Turowski, J. M., & Hovius, N. (2013). A demonstration of the importance of bedload transport for fluvial bedrock erosion and knickpoint propagation. *Earth Surface Processes and Landforms*, *38*(7), 683–695. https://doi.org/10.1002/esp.3313

Croissant, T., Lague, D., Steer, P., & Davy, P. (2017). Rapid post-seismic landslide evacuation boosted by dynamic river width. *Nature Geoscience*, *10*, 680.

Crossley, D., Hinderer, J., & Riccardi, U. (2013). The measurement of surface gravity. *Reports on Progress in Physics. Physical Society (Great Britain)*, *76*(4), 046101. https://doi.org/10.1088/0034-4885/76/4/046101

Dadson, S. J., Hovius, N., Chen, H., Dade, W. B., Hsieh, M. L., Willett, S. D., et al. (2003). Links between erosion, runoff variability and seismicity in the Taiwan orogen. *Nature*, *426*(6967), 648–651. Retrieved from http://dx.doi.org/10.1038/nature02150

Dadson, S. J., Hovius, N., Pegg, S., Dade, W. B., Horng, M. J., & Chen, H. (2005). Hyperpycnal river flows from an active mountain belt. *Journal of Geophysical Research: Earth Surface*, *110*(F4), n/a-n/a. https://doi.org/10.1029/2004JF000244

Darby, S. E., Hackney, C. R., Leyland, J., Kummu, M., Lauri, H., Parsons, D. R., et al. (2016). Fluvial sediment supply to a mega-delta reduced by shifting tropical-cyclone activity. *Nature*, *539*(7628), 276–279. https://doi.org/10.1038/nature19809

Deffontaines, B, Chang, K.-J., Champenois, J., Lin, K.-C., Lee, C.-T., Chen, R.-F., et al. (2018). Active tectonics of the onshore Hengchun Fault using UAS DSM combined with ALOS PS-InSAR time series (Southern Taiwan). *Nat. Hazards Earth Syst. Sci.*, *18*(3), 829–845. https://doi.org/10.5194/nhess-18-829-2018

Deffontaines, Benoît, Chang, K.-J., Champenois, J., Fruneau, B., Pathier, E., Hu, J.-C., et al. (2017). Active interseismic shallow deformation of the Pingting terraces (Longitudinal Valley – Eastern Taiwan) from UAV high-resolution topographic data combined with InSAR time series. *Geomatics, Natural Hazards and Risk*, *8*(1), 120–136. https://doi.org/10.1080/19475705.2016.1181678

Dehant, V., Defraigne, P., & Wahr, J. M. (1999). Tides for a convective Earth. *J. Geophys. Res.*, *104*, 1035–1058.

DeLisle, C., & Yanites, B. J. (2018). The impacts of landslides triggered by the 2009 Typhoon Morakot on landscape evolution: A mass balance approach. In *American Geophysical Union, Fall Meeting 2018, abstract #EP21C-2257* (Vol. 2018, pp. EP21C-2257). Retrieved from https://ui.adsabs.harvard.edu/abs/2018AGUFMEP21C2257D

Eltner, A., Kaiser, A., Castillo, C., Rock, G., Neugirg, F., & Abellán, A. (2016). Image-based surface reconstruction in geomorphometry – merits, limits and developments. *Earth Surf. Dynam.*, *4*(2), 359–389. https://doi.org/10.5194/esurf-4-359-2016

Farinotti, D., Longuevergne, L., Moholdt, G., Duethmann, D., Mölg, T., Bolch, T., et al. (2015). Substantial glacier mass loss in the Tien Shan over the past 50 years. *Nature Geoscience*, *8*(9), 716–722. https://doi.org/10.1038/ngeo2513

Ferguson, J. F., Klopping, F. J., Chen, T., Seibert, J. E., Hare, J. L., & Brady, J. L. (2008). The 4D microgravity method for waterflood surveillance: Part 3 — 4D absolute microgravity surveys at Prudhoe Bay, Alaska. *GEOPHYSICS*, *73*(6), WA163–WA171. https://doi.org/10.1190/1.2992510

Ferro, V., & Porto, P. (2000). Sediment Delivery Distributed (SEDD) Model. *Journal of Hydrologic Engineering*, *5*(4), 411–422. https://doi.org/10.1061/(ASCE)1084-0699(2000)5:4(411)

Fores, B., Champollion, C., Moigne, N. Le, & Chery, J. (2017). Impact of ambient temperature on spring-based relative gravimeter measurements. *Journal of Geodesy*, *91*(3), 269–277. https://doi.org/10.1007/s00190-016-0961-2

Fuller, C. W. W., Willett, S. D. D., Hovius, N., & Slingerland, R. (2003). Erosion rates for Taiwan mountain basins: new determinations from suspended sediment records and a stochastic model of their temporal variation. *J. Geol.*, *111*(1), 71–87. https://doi.org/10.1086/344665

Fuller, C. W. W., Willett, S. D. D., Fisher, D., & Lu, C. Y. Y. (2006). A thermomechanical wedge model of Taiwan constrained by fission-track thermochronometry. *Tectonophysics*, *425*(1–4), 1–24. https://doi.org/10.1016/j.tecto.2006.05.018

Ge, X., Li, T., Zhang, S., & Peng, M. (2010). What causes the extremely heavy rainfall in Taiwan during Typhoon Morakot (2009)? *Atmospheric Science Letters*, *11*(1), 46–50.

Gelaro, R., McCarty, W., Suárez, M. J., Todling, R., Molod, A., Takacs, L., et al. (2017). The Modern-Era Retrospective Analysis for Research and Applications, Version 2 (MERRA-2). *Journal of Climate*, *30*(14), 5419–5454. https://doi.org/10.1175/JCLI-D-16-0758.1

Han, S. C., Shum, C. K., Bevis, M., Ji, C., & Kuo, C.-Y. (2006). Crustal dilatation observed by GRACE after the 2004 Sumatra-Andaman earthquake. *Science (New York, N.Y.)*, *313*(5787), 658–663. https://doi.org/10.1126/science.1128661

Hare, J. L., Ferguson, J. F., & Brady, J. L. (2008). The 4D microgravity method for waterflood surveillance: Part IV — Modeling and interpretation of early epoch 4D gravity surveys at Prudhoe Bay, Alaska. *GEOPHYSICS*, *73*(6), WA173–WA180. https://doi.org/10.1190/1.2991120

Hartshorn, K., Hovius, N., Dade, W. B., & Slingerland, R. L. (2002). Climate-driven bedrock incision in an active mountain belt. *Science*, *297*(5589), 2036 LP – 2038. https://doi.org/10.1126/science.1075078

Hinderer, J., Crossley, D., & Warburton, R. J. (2015). Superconducting Gravimetry. In G. B. T.-T. on G. (Second E. Schubert (Ed.) (pp. 59–115). Oxford: Elsevier. https://doi.org/https://doi.org/10.1016/B978-0-444-53802-4.00062-2

Horowitz, A. J. (2003). An evaluation of sediment rating curves for estimating suspended sediment concentrations for subsequent flux calculations. *Hydrological Processes*, *17*(17), 3387–3409. https://doi.org/10.1002/hyp.1299

Horton, A. J., Constantine, J. A., Hales, T. C., Goossens, B., Bruford, M. W., & Lazarus, E. D. (2017). Modification of river meandering by tropical deforestation. *Geology*, *45*(6), 511–514. https://doi.org/10.1130/G38740.1

Hovius, N., Stark, C. P., Tsu, C. H., Chuan, L. J., Hao-tsu, C., Jiun-chuan, L., et al. (2000). Supply and removal of sediment in a landslide-dominated mountain belt: Central Range, Taiwan. *J. Geol.*, *108*(1), 73–89.

Hovius, N., Meunier, P., Lin, C.-W., Chen, H., Chen, Y.-G. G., Dadson, S. J., et al. (2011). Prolonged seismically induced erosion and the mass balance of a large earthquake. *Earth Planet. Sci. Lett.*, *304*(3), 347–355. https://doi.org/10.1016/j.epsl.2011.02.005

Hsieh, M.-L., & Capart, H. (2013). Late Holocene episodic river aggradation along the Lao-nong River (southwestern Taiwan): An application to the Tseng-wen Reservoir Transbasin Diversion Project. *Engineering Geology*, *159*, 83–97. https://doi.org/https://doi.org/10.1016/j.enggeo.2013.03.019

Huang, M. Y.-F., & Montgomery, D. R. (2013). Altered regional sediment transport regime after a large typhoon, southern Taiwan. *Geology* . https://doi.org/10.1130/G34826.1

Hwang, C., Wang, C. G., & Lee, L. H. (2002). Adjustment of relative gravity measurements using weighted and datum-free constraints. *Computers and Geosciences*, *28*(9), 1005–1015.

IES-AS. (2015). GPS LAB. Retrieved from http://gps.earth.sinica.edu.tw/

Jaboyedoff, M., Oppikofer, T., Abellán, A., Derron, M. H., Loye, A., Metzger, R., & Pedrazzini, A. (2012, March). Use of LIDAR in landslide investigations: A review. *Natural Hazards*. https://doi.org/10.1007/s11069-010-9634-2

Jacob, T., Chery, J., Bayer, R., Le Moigne, N., Boy, J.-P., Vernant, P., & Boudin, F. (2009). Time-lapse surface to depth gravity measurements on a karst system reveal the dominant role of the epikarst as a water storage entity. *Geophysical Journal International*, *177*(2), 347–360. https://doi.org/10.1111/j.1365-246X.2009.04118.x

Jacob, T., Bayer, R., Chery, J., & Le Moigne, N. (2010). Time-lapse microgravity surveys reveal water storage heterogeneity of a karst aquifer. *Journal of Geophysical Research*, *115*(B6), B06402. https://doi.org/10.1029/2009JB006616

Kao, R., Hwang, C., Kim, J. W., Ching, K.-E., Masson, F., Hsieh, W.-C., et al. (2017). Absolute gravity change in Taiwan: Present result of geodynamic process investigation. *Terrestrial, Atmospheric & Oceanic Sciences*, *28*(6), 855–875.

Kazama, T., Okubo, S., Sugano, T., Matsumoto, S., Sun, W., Tanaka, Y., & Koyama, E. (2015). Absolute gravity change associated with magma mass movement in the conduit of Asama Volcano (Central Japan), revealed by physical modeling of hydrological gravity disturbances. *J. Geophys. Res.*, 1263–1287. https://doi.org/10.1002/2014JB011563

Letellier, T., Lyard, F., & Lefèvre, F. (2004). The new global tidal solution: FES2004. In *Proceedings of the Ocean Surface Topography Science Team Meeting, St. Petersburg, Florida* (pp. 4–6).

Lin, C.-W., Chang, W.-S., Liu, S.-H., Tsai, T.-T., Lee, S.-P., Tsang, Y.-C., et al. (2011). Landslides triggered by the 7 August 2009 Typhoon Morakot in southern Taiwan. *Engineering Geology*, *123*(1), 3–12. https://doi.org/https://doi.org/10.1016/j.enggeo.2011.06.007

Lin, G.-W., & Chen, H. (2013). Recurrence of hyper-concentration flows on the orogenic, subtropical island of Taiwan. *Journal of Hydrology*, *502*, 139–144. https://doi.org/10.1016/J.JHYDROL.2013.08.036

Liu, H., & Pike, W. T. (2016). A micromachined angular-acceleration sensor for geophysical applications. *Applied Physics Letters*, *109*(17), 173506. https://doi.org/10.1063/1.4966547

Liu, Y.-C., Hwang, C., Han, J., Kao, R., Wu, C.-R., Shih, H.-C., & Tangdamrongsub, N. (2016). Sediment-Mass Accumulation Rate and Variability in the East China Sea Detected by GRACE. *Remote Sensing*, *8*(10), 777. https://doi.org/10.3390/rs8090777

Longuevergne, L., Boy, J.-P., Florsch, N., Viville, D., Ferhat, G., Ulrich, P., et al. (2009). Local and global hydrological contributions to gravity variations observed in Strasbourg. *J. Geodyn.*, *48*(3–5), 189–194. https://doi.org/10.1016/j.jog.2009.09.008

Longuevergne, L., Wilson, C. R., Scanlon, B. R., & Crétaux, J. F. (2013). GRACE water storage estimates for the middle east and other regions with significant reservoir and lake storage. *Hydrology and Earth System Sciences*, *17*(12), 4817–4830. https://doi.org/10.5194/hess-17-4817-2013

Ménoret, V., Vermeulen, P., Le Moigne, N., Bonvalot, S., Bouyer, P., Landragin, A., & Desruelle, B. (2018). Gravity measurements below 10-9g with a transportable absolute quantum gravimeter. *Scientific Reports*, *8*(1), 1–11. https://doi.org/10.1038/s41598-018-30608-1

Merriam, J. B. (1992). Atmospheric pressure and gravity. *Geophysical Journal International*, *109*(3), 488–500. https://doi.org/10.1111/j.1365-246X.1992.tb00112.x

Middlemiss, R. P., Samarelli, A., Paul, D. J., Hough, J., Rowan, S., & Hammond, G. D. (2016). The first measurement of the Earth tides with a MEMS gravimeter. *Nature*, *531*, 614–617. https://doi.org/10.1038/nature17397

Middlemiss, R. P., Bramsiepe, S. G., Douglas, R., Hough, J., Paul, D. J., Rowan, S., & Hammond, G. D. (2017). Field tests of a portable MEMS gravimeter. *Sensors (Switzerland)*, *17*(11), 1–12. https://doi.org/10.3390/s17112571

Milliman, J. D., & Farnsworth, K. L. (2011). *River Discharge to the Coastal Ocean: A Global Synthesis*. *Cambridge University Press*.

Molnar, P., Anderson, R. S., & Anderson, S. P. (2007). Tectonics, fracturing of rock, and erosion. *Journal of Geophysical Research: Earth Surface*, *112*(3), 1–12. https://doi.org/10.1029/2005JF000433

Morera, S. B., Condom, T., Crave, A., Steer, P., & Guyot, J. L. (2017). The impact of extreme El Niño events on modern sediment transport along the western Peruvian Andes (1968–2012). *Scientific Reports*, *7*(1), 11947. https://doi.org/10.1038/s41598-017-12220-x

Mouyen, M., Masson, F., Hwang, C., Cheng, C.-C., Le Moigne, N., Lee, C. W., et al. (2013). Erosion effects assessed by repeated gravity measurements in southern Taiwan. *Geophysical Journal International*, *192*(1), 113–136. https://doi.org/10.1093/gji/ggs019

Mouyen, M., Longuevergne, L., Steer, P., Crave, A., Lemoine, J. M., Save, H., & Robin, C. (2018). Assessing modern river sediment discharge to the ocean using satellite gravimetry. *Nature Communications*, *9*(1), 3384. https://doi.org/10.1038/s41467-018-05921-y

Nagy, D. (1966). The prism method for terrain corrections using digital computers. *Pure and Applied Geophysicseophysics*, *63*(1), 31–39. https://doi.org/10.1007/BF00875156

Naujoks, M., Weise, A., Kroner, C., & Jahr, T. (2008). Detection of small hydrological variations in gravity by repeated

observations with relative gravimeters. *Journal of Geodesy*, *82*(9), 543–553. https://doi.org/10.1007/s00190-007-0202-9

Niebauer, T. M. (2015). Gravimetric methods – absolute gravimeter : instruments concepts and implementation. In G. Schubert (Ed.), *Treatise on Geophysics* (Vol. 3, pp. 37–57). Elsevier.

Niebauer, T. M., Sasagawa, G. S., Faller, J. E., Hilt, R., & Klopping, F. (1995). A new generation of absolute gravimeters. *Metrologia*, *32*, 159–180.

Niethammer, U., James, M. R., Rothmund, S., Travelletti, J., & Joswig, M. (2012). UAV-based remote sensing of the Super-Sauze landslide: Evaluation and results. *Engineering Geology*, *128*, 2–11. https://doi.org/https://doi.org/10.1016/j.enggeo.2011.03.012

Pail, R., Bingham, R., Braitenberg, C., Dobslaw, H., Eicker, A., Güntner, A., et al. (2015). Science and user needs for observing global mass transport to understand global change and to benefit society. *Surveys in Geophysics*, *36*(6), 743–772. https://doi.org/10.1007/s10712-015-9348-9

Peizhen, Z., Molnar, P., & Downs, W. R. (2001). Increased sedimentation rates and grain sizes 2-4 Myr ago due to the influence of climate change on erosion rates. *Nature*, *410*(April), 891–897. https://doi.org/10.1038/35073504

Petrov, L., & Boy, J.-P. (2004). Study of the atmospheric pressure loading signal in very long baseline interferometry observations. *Journal of Geophysical Research*, *109*(B3), B03405. https://doi.org/10.1029/2003JB002500

Pfeffer, J., Champollion, C., Favreau, G., Cappelaere, B., Hinderer, J., Boucher, M., et al. (2013). Evaluating surface and subsurface water storage variations at small time and space scales from relative gravity measurements in semiarid Niger. *Water Resources Research*, *49*(6). https://doi.org/10.1002/wrcr.20235

Rebischung, P., Griffiths, J., Ray, J., Schmid, R., Collilieux, X., & Garayt, B. (2012). IGS08: The IGS realization of ITRF2008. *GPS Solutions*, *16*(4), 483–494. https://doi.org/10.1007/s10291-011-0248-2

Rodell, M., Houser, P. R., Jambor, U., Gottschalck, J., Mitchell, K., Meng, C.-J. J., et al. (2004). The Global Land Data Assimilation System. *Bulletin of the American Meteorological Society*, *85*(3), 381–394. https://doi.org/10.1175/BAMS-85-3-381

Schwab, M., Rieke-Zapp, D., Schneider, H., Liniger, M., & Schlunegger, F. (2008). Landsliding and sediment flux in the Central Swiss Alps: A photogrammetric study of the Schimbrig landslide, Entlebuch. *Geomorphology*, *97*(3), 392–406. https://doi.org/https://doi.org/10.1016/j.geomorph.2007.08.019

Scintrex Ltd. (2010). *CG-5 Scintrex Autograv System, Operation Manual*. Scintrex Limited, Concord, Ontario, Canada, http://www.scintrexltd.com/.

Steer, P., Huismans, R. S., Valla, P. G., Gac, S., & Herman, F. (2012). Bimodal plio-quaternary glacial erosion of fjords and low-relief surfaces in Scandinavia. *Nature Geoscience*, *5*(9), 635–639. https://doi.org/10.1038/ngeo1549

Steer, P., Simoes, M., Cattin, R., & Shyu, J. B. H. (2014). Erosion influences the seismicity of active thrust faults. *Nature Communications*, *5*, 5564. https://doi.org/10.1038/ncomms6564

Taiwan Water Resources Agency. (2019). Hydrological Year Book of Taiwan Republic of China. Retrieved from

http://gweb.wra.gov.tw/wrhygis/

Tapley, B. D., Bettadpur, S., Ries, J. C., Thompson, P. F., & Watkins, M. M. (2004). GRACE measurements of mass variability in the Earth system. *Science (New York, N.Y.)*, *305*(5683), 503–5. https://doi.org/10.1126/science.1099192

Torres, A., Brandt, J., Lear, K., & Liu, J. (2017). A looming tragedy of the sand commons. *Science (New York, N.Y.)*, *357*(6355), 970–971. https://doi.org/10.1126/science.aao0503

Tu, J. T., Chou, C., & Chu, P. S. (2009). The abrupt shift of typhoon activity in the vicinity of Taiwan and its association with western North Pacific-East Asian climate change. *Journal of Climate*, *22*(13), 3617–3628. https://doi.org/10.1175/2009JCLI2411.1

Walling, D. E., & Fang, D. (2003). Recent trends in the suspended sediment loads of the world's rivers. *Global and Planetary Change*, *39*(1), 111–126. https://doi.org/https://doi.org/10.1016/S0921-8181(03)00020-1

Wessel, P., Smith, W. H. F., Scharroo, R., Luis, J., & Wobbe, F. (2013). Generic Mapping Tools: Improved Version Released. *Eos, Transactions American Geophysical Union*, *94*(45), 409–410. https://doi.org/10.1002/2013EO450001

Willett, S. D. (1999). Orogeny and orography: The effects of erosion on the structure of mountain belts. *J. Geophys. Res.*, *104*(B12), 28,957-28,981. https://doi.org/10.1029/1999JB900248

Appendix A: Processing of the relative gravity survey

Figures A1, A2 and A3 summarize how each relative survey were done in 2015, 2016 and 2017, respectively. All relative loops start and end at AG06 and other relative gravity sites (prefix BA) are re-measured several time for each survey, within a few hours. It is necessary to have such repeated measures in order to estimate and remove the instrumental drift of the CG5 relative gravimeter. The adjustment is done using the software Gravnet (Hwang et al., 2002), assuming drift linear with time. The instrumental drift for each year are:

2015: 0.032 ± 0.037 mGal day^{-1}

2016: -0.085±0.004 mGal day^{-1}

2017: -0.161±0.007 mGal day^{-1}

Formatted: Level 1

Formatted: Superscript

Formatted: Superscript

Formatted: Superscript

Formatted: Caption

Appendix B: Gravimetric effect of the dolosse

Fig. B1a is a picture of the dolosse stacked near the gravity site BA02. Their side L and height H are reported with blue lines for comparison with Figs. B1c-d. They are made of 3 identical patterns, which repeats around the center of the dolosse, and close it. The center of the dolosse and part of his sides are empty. However, due to its limited spatial resolution, the photogrammetry "sees" the dolosse as plain hexagons (Fig. B1b). Our aim is thus to define the ratio k between an actual dolosse and a plain dolosse. This ratio is then multiplied by the average density ρ_c of concrete (2.3×10^3 kg m^{-3}), which the dolosse are made of. This way we obtain an effective dolosse density that we pair to the volume obtained from the photogrammetry and eventually compute the gravitational effect of the dolosse at our study sites.

The volume Vp of a regular hexagon with side L and height H is

$$V = \frac{3}{2}\sqrt{3}L^2H = 4.9 \text{ m}^3 \quad \text{(A1)}$$

The volume Vd of the actual dolosse is estimated to 1.6 m^3, using the geometry detailed in Figs. B1c-d. Therefore, we find that the true volume of the dolosse is $k = 1.6/4.9 \cong 0.33$, that is one third of the plain volume, hence its effective density is $2.3k = 0.76\times10^3$ kg m^{-3}. The geometry and density of the dolosse were used to compute their gravitational attraction at BA04 and BA05 using a gravity modelling by rectangular prisms methods (Nagy, 1966). This effect is about -15 µGal.

Deleted: A

Deleted: A

Deleted: A

Deleted: A

Deleted: A

Deleted: a 3-dimensionnal (3D)

Appendix C: In situ determination of the river materials density

Site selection:

We select 20 sites in the active river channel, which are accessible by walking. We try to find sites where materials are different, some of them being close to each other, to better grasp the variety of the material in the channel. Nevertheless, we also try to have a spatially even sampling. In a few places, two sampling are done at the same horizontal position but at the surface and then deeper. All sites positions are recorded with a hand gps (about 3 m accuracy).

Material sampling

At each start, we first distribute several benchmarked rules all around the place that will be sampled (Fig. C1a). Several pictures are taken to cover the sampling site and several benchmarked rules at a time. Pictures should overlap each other. We then dig a hole of about 30- 40cm depth and radius, paying attention to not move any of the benchmarked rules. The excavated material M is put in a bucket of known mass and weighted using a hook-hanging weight machine. Then another set of pictures is taken to cover again the benchmarked rules and the hole just dug. The only difference between the pictures taken before and after is the hole.

Photogrammetry:

The benchmarked rules make a common reference between the pictures taken before and after the hole is dug. They are transformed into clouds of points in 3D (Fig. C1b), one representing the original surface, the other representing the dug surface. Thus, subtracting these two surfaces returns the surface of the hole, from which the volume V of the hole is computed (Fig. C1c).

Density computation:

The density at the sampling site is then M divide by V.

Deleted: B

Deleted: and divide it by the volume to get a density. bucket

Deleted: The volume of the hole is evaluated by photogrammetry (Fig. B1).

Deleted: Weight the The excavated material is put in a bucket.The in situ densities were determined in three steps

Deleted: Dig a small hole in the material (30-40 cm depth).

Tables

Effect	Method	Order of magnitude [µGal]	Uncertainty [µGal]	Correction applied
Solid earth tides	WDD	100	0.1	Before the adjustment
Ocean tide loading	FES 2004 model	10	0.1	Before the adjustment
Polar motions	IERS data	1	0.1	Before the adjustment
Air pressure	Barometer data	0.5-1	0.1	Before the adjustment
Vertical ground motions	GNSS data	-2-4	1-2	After the adjustment
Hydrology	GLDAS2/MERRA2 model	2	5	After the adjustment
Dolosse at BA03, BA04	Photogrammetry	-15	5	After the adjustment

Table 1: Summary of the corrections applied to our gravity measurements, with their order of magnitude and a statement on whether there are applied before or after the drift adjustment. The uncertainties on the first four corrections are those proposed by Van Camp et al., 2005.

Site	2015	2016	2017
AG06	978713849.3 ± 1.6	978713845.2 ± 0.9	978713845.7 ± 3
BA01	-795.7 ± 1.3	-793.7 ± 1.8	-799.9 ± 1.8
BA02	-474.5 ± 2.1	-489.9 ± 2.0	No value
BA03	-204.9 ± 2.6	-176.7 ± 2.0	-217.2 ± 6.6
BA04	292.8 ± 2.4	347.3 ± 2.3	300.5 ± 6.8
BA05	673.8 ± 2.6	715.1 ± 2.3	718.8 ± 1.4
BA06	901.9 ± 2.4	960.6 ± 2.4	965.6 ± 1.4
BA07	1188.8 ± 2.4	1254.4 ± 2.4	1240.8 ± 1.5
BA08	1637.7 ± 2.1	1666.2 ± 2.2	1653.7 ± 1.8
BA09	1932.4 ± 1.4	1928.0 ± 2.8	1906.5 ± 1.3

Table 2: Gravity values measured at each site for all surveys, in microGal. The values at each relative gravity site (BA) are given relative to the absolute value measured at AG06.

Formatted: Swedish (Sweden)

Case	Densities (10^3 kg m^{-3})		RMS (µGal)
	River	Landslide	
1	ρ = 1.9 ± 0.01 (no distinction river/landslide)		9.6
2	ρ_r = 1.9 ± 0.01	ρ_l = 2.0 ± 0.1	9.5
3	ρ_r^{1615} = 1.6 ± 0.1 ; ρ_r^{1716} = 2.0 ± 0.01	ρ_l = 1.7 ± 0.3	9.6

Table 3: Densities obtained for each inversion case, with their standard deviation and the root mean square of the residuals *V*.

Deleted: 2

Figures

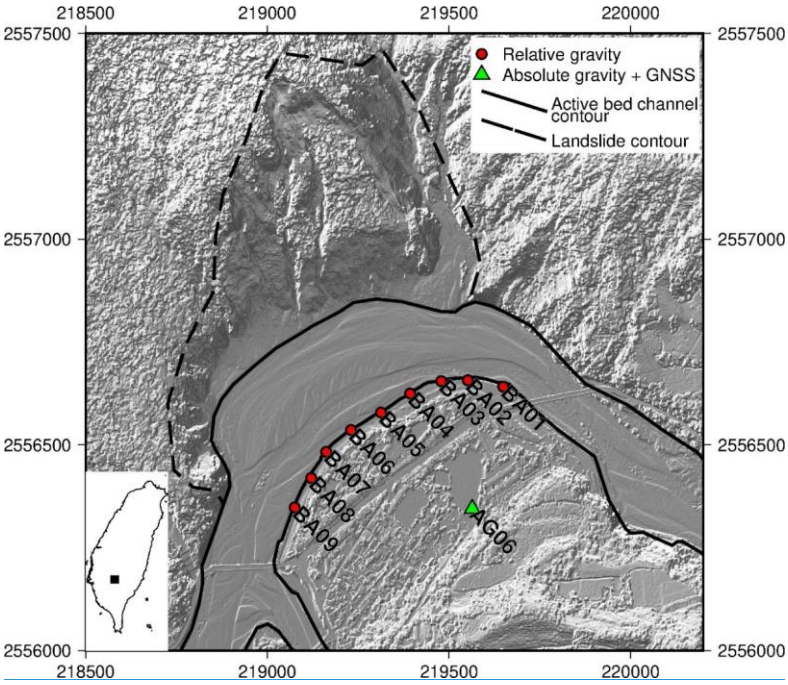

Figure 1: Map of the study area. Absolute gravity measurements are performed only at AG06 while relative gravity measurements are performed at every site. The background image is the hillshaded topography at half-meter resolution obtained by photogrammetry using an unmanned aerial vehicle (UAV). Inset in the left panel shows the study area in Taiwan. Axis are in meters.

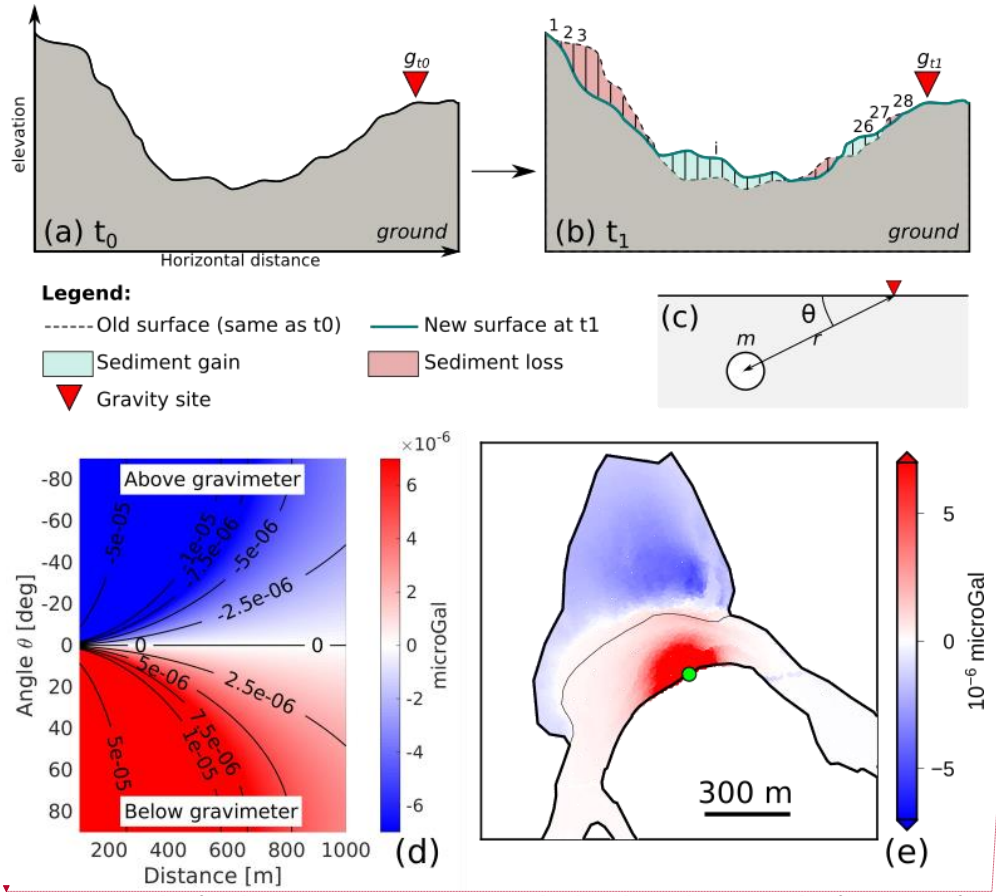

Figure 2: a) Ground surface elevation at time t_0, gravity is measured and equal to g_{t0}. b) New ground surface at $t_1 > t_0$, after sediment mass redistributions occurred. The gravity is measured again at the same place and is equal to g_{t1}. c) Parameters used for computing a point-mass gravity effect (equation 1, point-mass means that the element is approximated to a point which mass is that of the element). d) Theoretical effect of a 2000-kg point mass as a function to its distance and angle (Eq. 1) from the gravimeter. e) Synthetic gravity effect at one measurement site (green dot, actually BA04) for each mass element located at the surface of the Paolai river bed or landslide. A mass element is a 0.5x0.5x1 m rectangular prisms of density 2, which height is given by the actual topography of the area (Fig. 1). The actual gravity effect measured at the green site is the sum of each element gravity effect. The colorscale is saturated to highlight the change of sign across the landslide area.

Deleted: <object>

Deleted: 1

945

Deleted: **Figure 2: Map of the study area. Absolute gravity measurements are performed only at AG06 while relative gravity measurements are performed at every site. The background image is the hillshaded topography at half-meter resolution obtained by photogrammetry using an unmanned aerial vehicle (UAV). Inset in the left panel shows the study area in Taiwan. Axis are in meters.**

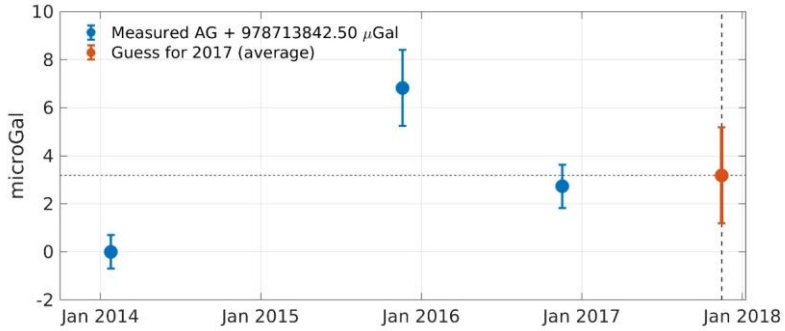

Figure 3: Absolute gravity values measured at AG06 in 2014 (January 25), 2015 (November 20) and 2016 (November 18). In 2017 (November 16), the absolute gravimeter suffered from a laser problem and no measurement could be done. We thus consider that the value in 2017 is the average of the 2014, 2015 and 2016 values. These absolute gravity values are already corrected for tides, air pressure and polar motions, but not for hydrology and vertical ground displacements yet. The error bar for the values in 2014, 2015 and 2016 combine the measurement uncertainty obtained during each a gravity survey and the uncertainties due to the tides, air pressure and polar motions corrections.

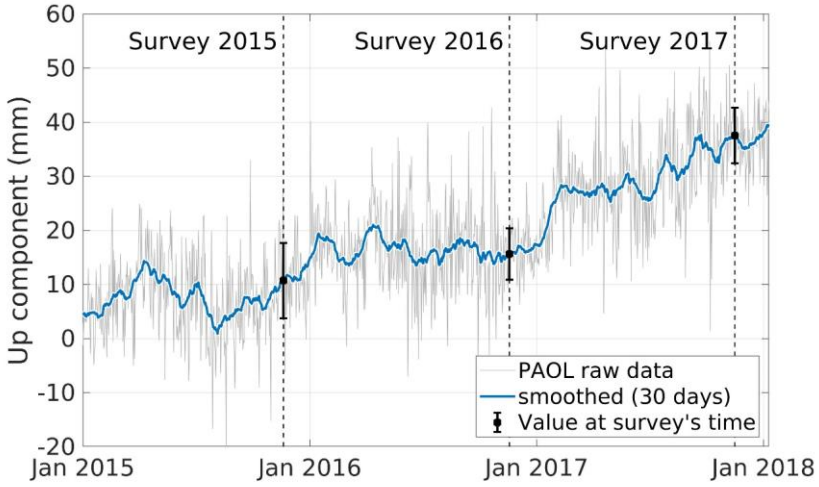

965

Figure 4: Ground vertical displacements time series at PAOL GNSS station, co-located with AG06, provided by the GPSLAB database (IES-AS, 2015)**. Solutions are computed in the IGS08 reference frame** (Rebischung et al., 2012)**. The time of each joined gravity and photogrammetry survey is shown by dotted lines. The error bar is computed from the standard deviation of the measurements of the same 30-days window.**

970

Deleted: P

Deleted: l

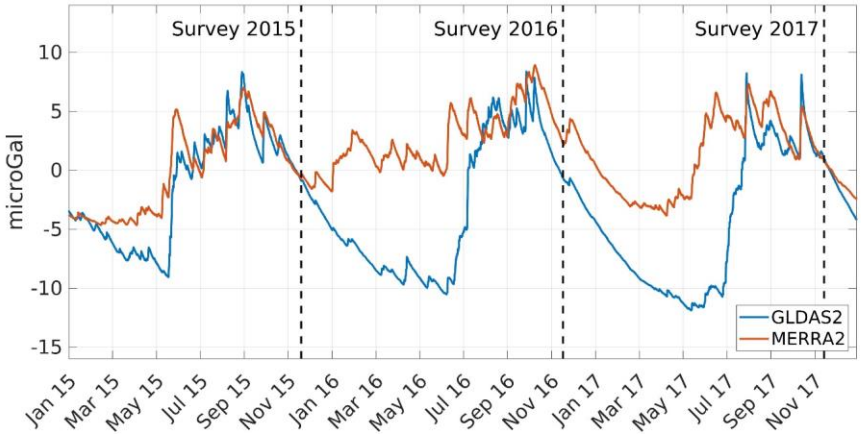

975 **Figure 5: Hydrological effect on gravity at AG06, estimated from global hydrological models GLDAS2 and MERRA2.**

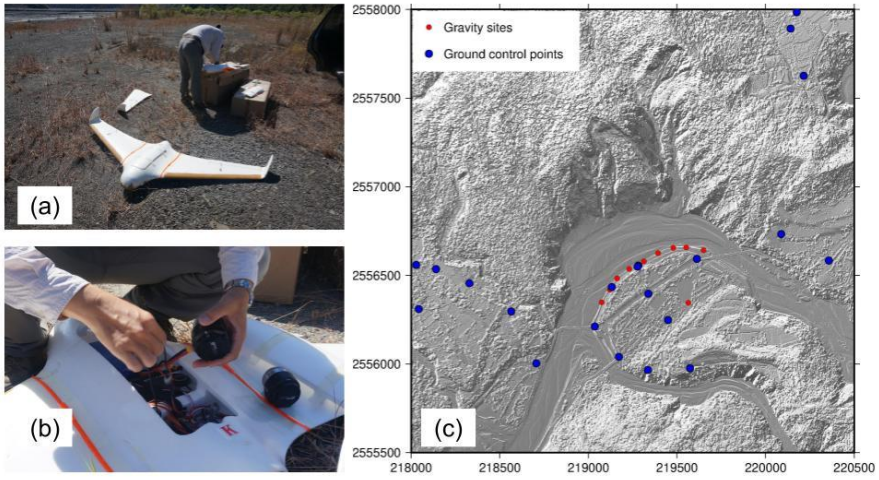

Figure 6: a) UAV, modified Skywalker X8. b) Close-up on the central compartment of the UAV, where the camera and lens are mounted. c) Map of the ground control points with the shaded topography in the background. The gravity sites are also shown for reference.

985

Deleted: **Figure 7: Gravity changes between (a) 2015 and 2016 and (b) between 2016 and 2017. BA02 could not be measured in 2017 because of construction work ongoing near the site. The error bars represent**  **where σ's are the uncertainties of the gravity measurements and of the seven corrections given in Table 1 (thus i ranges from 1 to 8).**

995

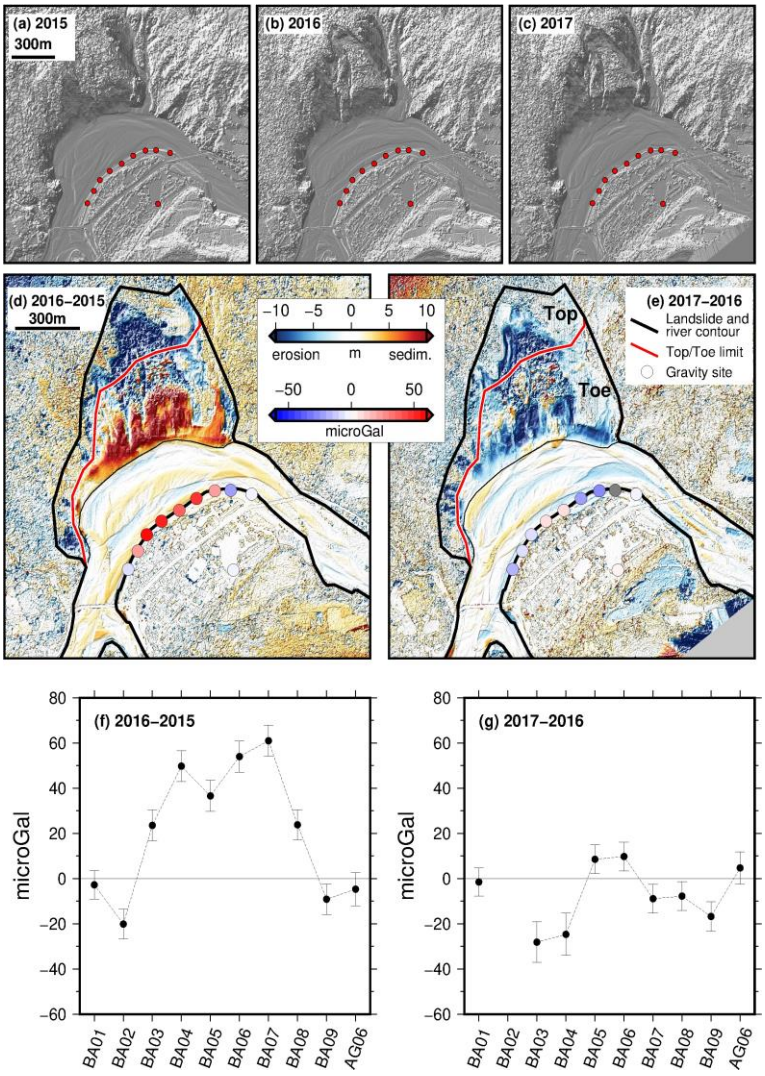
(a) 2015
300m
(b) 2016
(c) 2017
(d) 2016–2015
300m
−10 −5 0 5 10
erosion m sedim.
−50 0 50
microGal
(e) 2017–2016
Landslide and river contour
Top/Toe limit
Gravity site
Top
Toe
(f) 2016–2015
(g) 2017–2016
microGal
80
60
40
20
0
−20
−40
−60
BA01
BA02
BA03
BA04
BA05
BA06
BA07
BA08
BA09
AG06

Figure 7: The digital surface models in a) 2015, b) 2016 and c) 2017 and their differences d) between 2016 and 2015 and e) between 2017 and 2016. The disks that locate the gravity sites are colored relative to the gravity change. The black contour line limits the river and the landsliding area. The landsliding area is divided into two parts: the top and the toe. The color scale of the elevation changes is bounded within ±10 m, which contains 92% of the elevation changes between 2015 and 2016, and 96% of the elevation changes between 2016 and 2017. The extrema are -46 m/33 m between 2015 and 2016, and -38 m/33 m between 2016 and 2017. (f) Gravity changes between 2015 and 2016 . (g) Gravity changes between 2016 and 2017. BA02 could not be measured in 2017 because of construction work ongoing near the site. The error bars represent $\sqrt{\sum_i \sigma_i^2}$ where σ's are the uncertainties of the gravity measurements after the instrumental drift adjustment and of the seven corrections given in Table 1 (thus i ranges from 1 to 8).

Deleted: 8

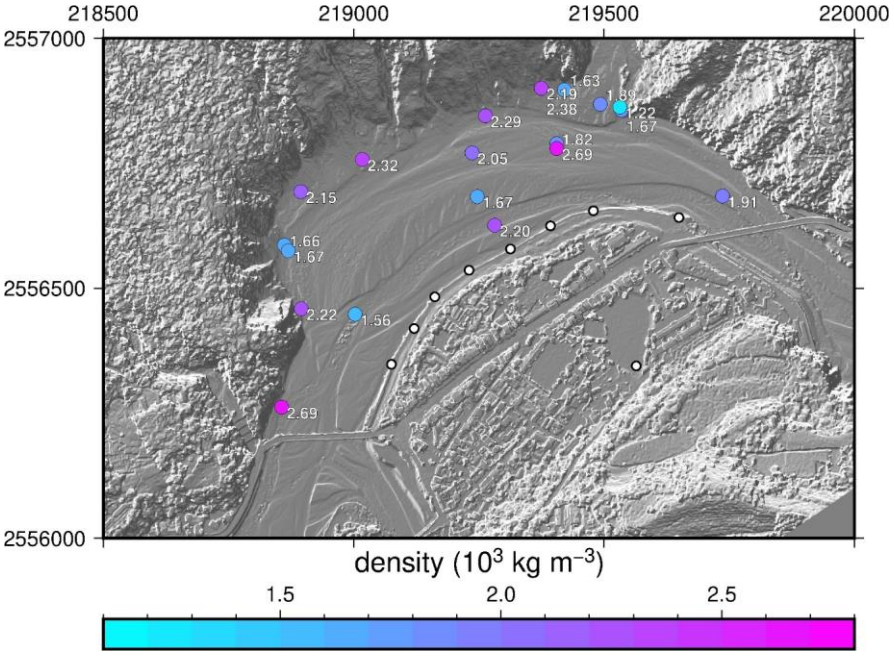

Figure 8: In situ density measured during the 2017 survey (colored dots, the value is also reported in white). Gravity sites are shown with white dots. Axes are in meters. The background is the shaded topography measured during the 2017 survey.

Deleted: 9

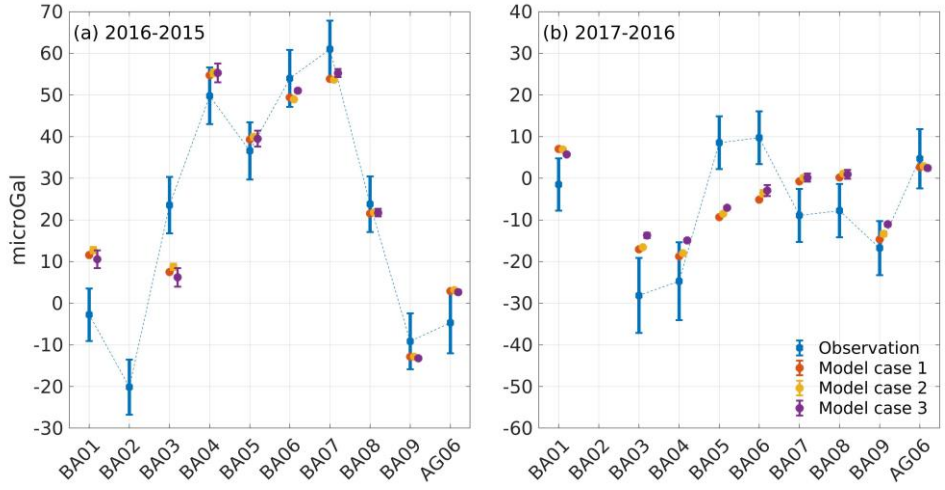

Figure 9: Comparison of the observed (blue) and modelled gravity changes for the densities inverted in cases 1, 2 and 3 (red, yellow and purple, respectively). Each case is slightly offset horizontally for legibility. No gravity is estimated at BA02 since its location is unknown.

Deleted: 10

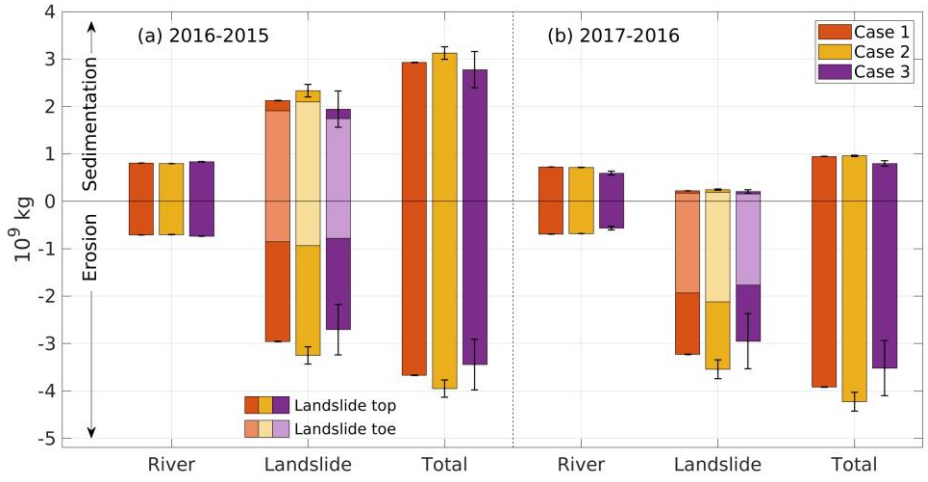

Figure 10: Estimation of the mass of sediment redistributed between 2016 and 2015, and between 2017 and 2016 in cases 1, 2 and 3 (red, yellow and purple, respectively; same color code as in Fig. 9). The mass estimation is shown for the river, the landslide and their sum (total). The error bars are computed by multiplying the volumes variations from the DSM with the densities uncertainties (Table 3). The landslide volumes distinguish the top and the toe of the landslides with a stacked bar plot form.

Deleted: 1

Deleted: 10

Deleted: 2

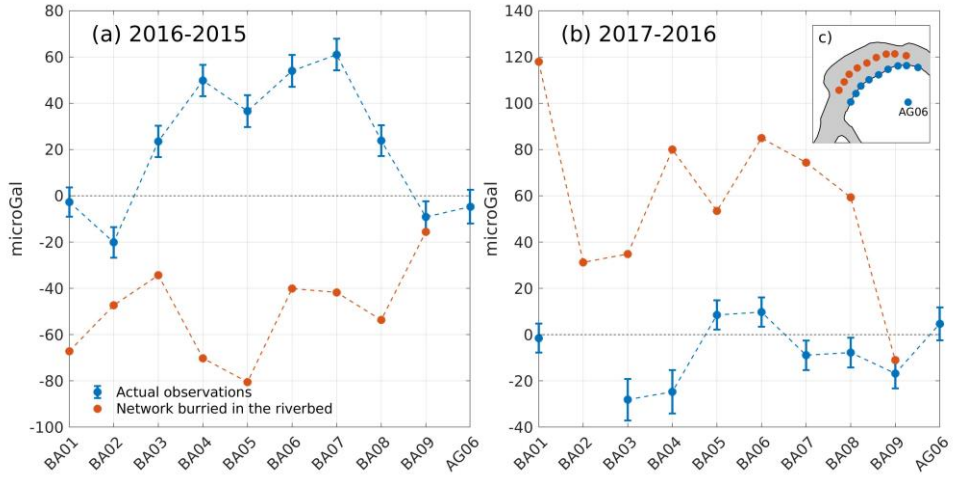

Figure 11: Gravity changes expected at new sites located 5 m beneath the river (red), compared with those measured at BA01-BA09 (blue), for the same sediment mass redistributions as a) between 2015 and 2016 and b) between 2016 and 2017. The new sites are in fact BA01 – BA09 translated 140 m in the north-east direction, as illustrated in c).

Deleted: 2

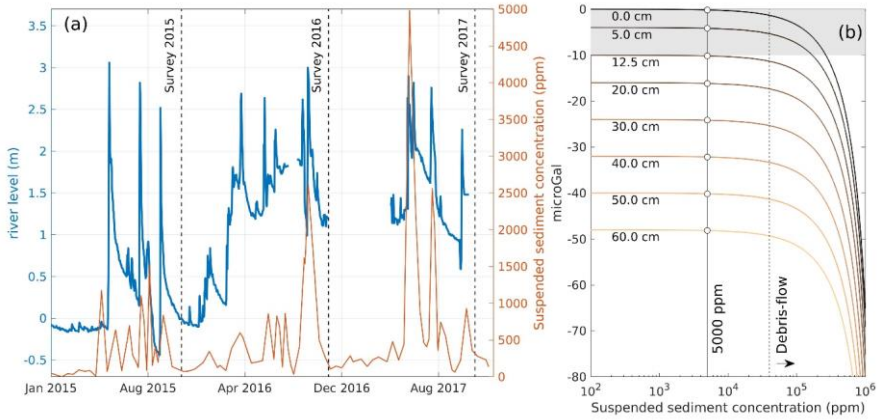

Figure 12: a) River level and sediment concentration of Laonong River, measured at LiuGui station, about 20 km downstream from Paolai. The highest sediment concentration (5000 ppm) is reached in summer 2017, when the river level increased by about 1.6 m. Data are freely available at the Taiwan WRA (Taiwan Water Resources Agency, 2019)**. b) Estimated gravity changes at the buried network (Fig. 11c) as a function of the suspended sediment load and of increasing amounts of bedload-transported sediment. The bedload fraction is considered here as a homogenous layer of 0 to 60 cm thickness (labelled on each curve) and density 2×10^3 kg m^{-3}. The river becomes a debris-flow when its suspended sediment concentration goes beyond 4×10^4 ppm. The 5000 ppm level is shown as a reference. Note that the gravity sign is negative because the mass is increased above the gravimeters.**

Deleted: 3

Deleted: 2

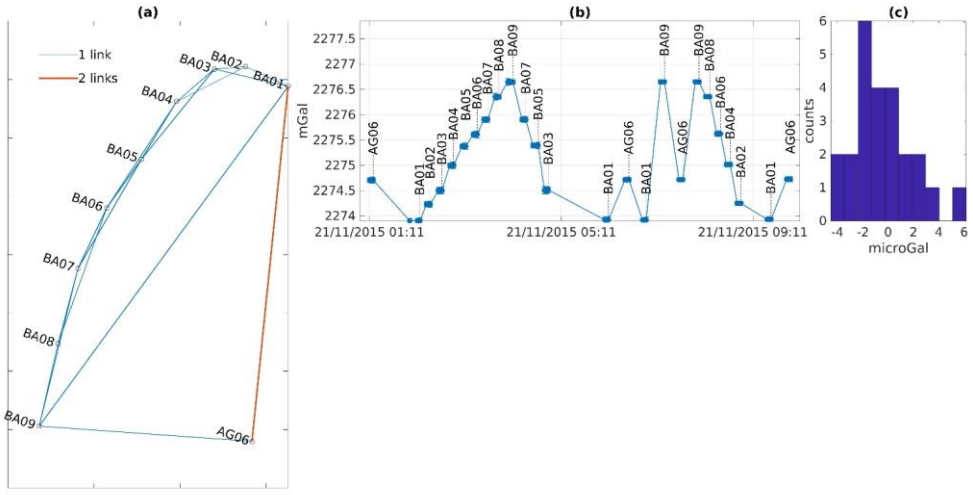

Figure A1: (a) Map view of the relative gravity network with the link between each site for the 2015 survey. (b) Gravity readings on the CG5 at each site as a function of time. (c) Histogram of the residuals after the drift adjustment.

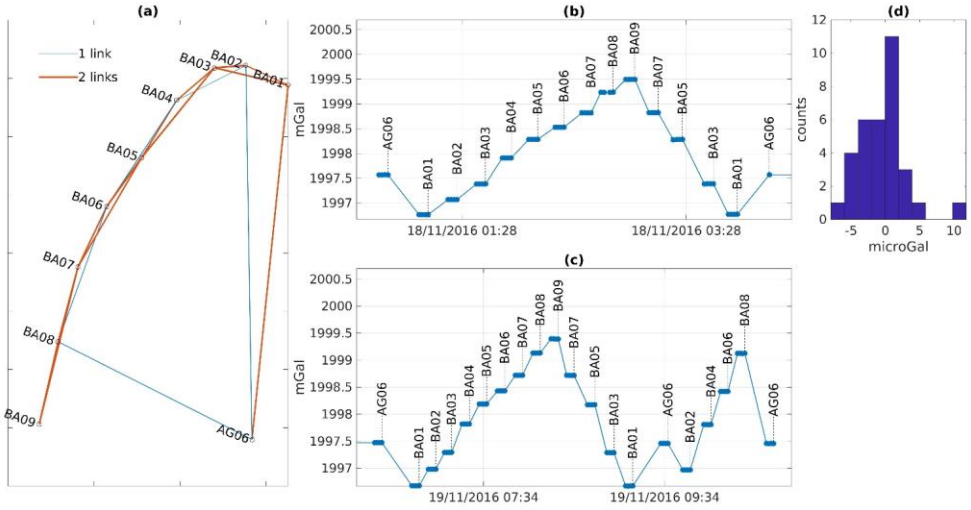

Figure A2: (a) Map view of the relative gravity network with the link between each site for the 2016 survey. (b) and (c) Gravity readings on the CG5 at each site as a function of time. (d) Histogram of the residuals after the drift adjustment.

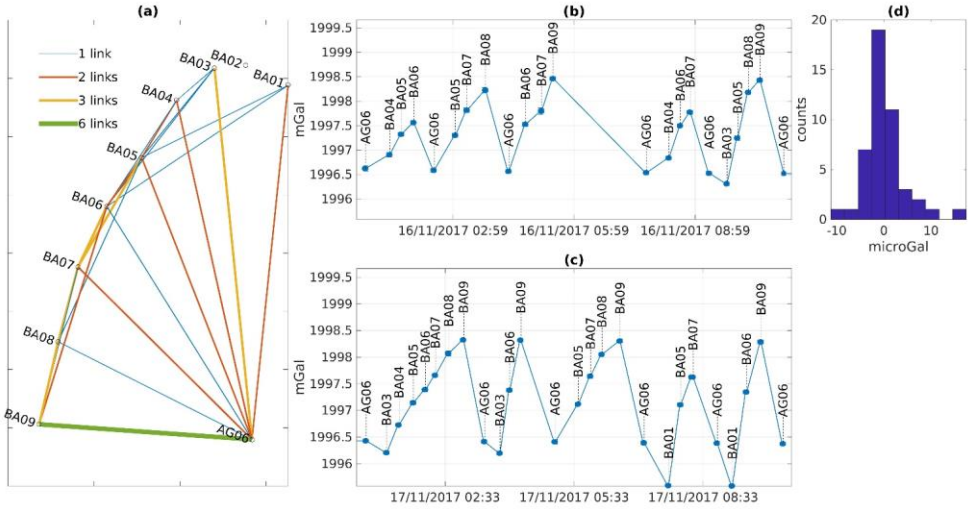

Figure A3: (a) Map view of the relative gravity network with the link between each site for the 2017 survey. (b) and (c) Gravity readings on the CG5 at each site as a function of time. (d) Histogram of the residuals after the drift adjustment.

Formatted: Normal

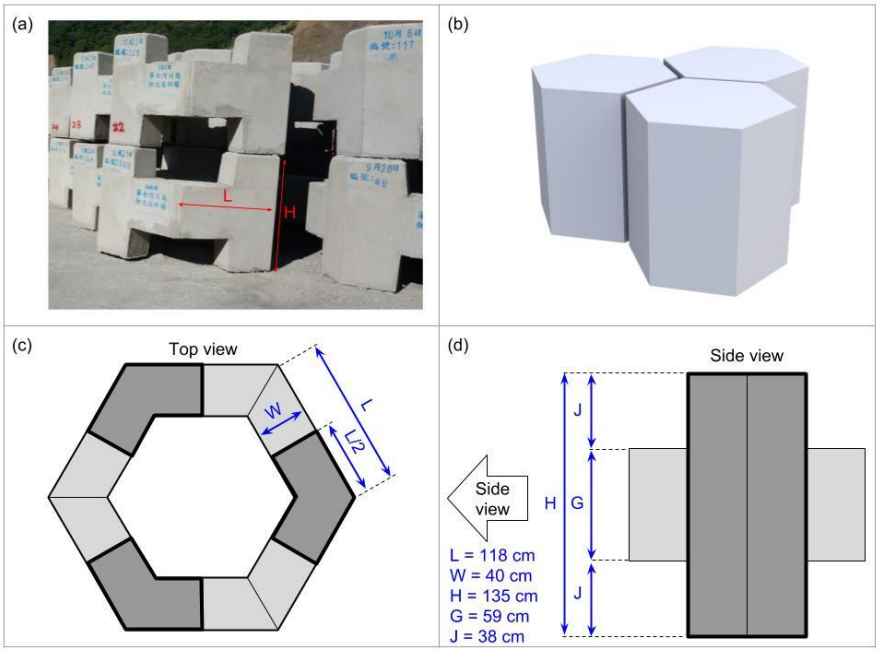

Figure B1: a) Photography of the dolosse. b) 3D hexagonal shape of the plain dolosse, as seen by the photogrammetry. c) Top view of the actual dolosse. The dark gray parts are the pillars actually touching the ground and the light gray parts are the "arms" of the dolosse. d) Side view of one dolosse element. One dolosse consists in three of these parts, joined by the arms.

Deleted: A

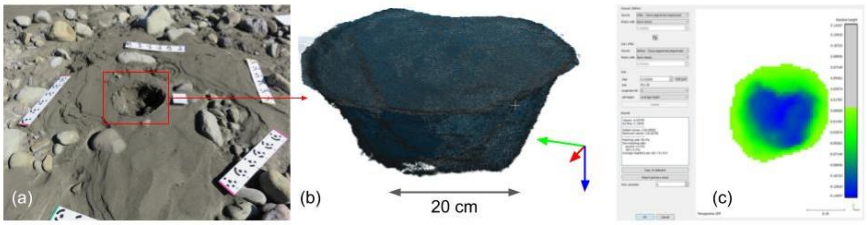

Figure C1: a) Picture of the hole taken with references scales and benchmarks. Several pictures were thus taken before and after the hole was dug. b) 3D cloud of the points mapping the surface of the hole. c) Computation of the volume bounded by the hole and the former surface of the ground, before the hole was done.

Deleted: B

Deleted: hole